INTERNATIONAL ATOMIC ENERGY AGENCY
UNITED NATIONS EDUCATIONAL, SCIENTIFIC AND CULTURAL ORGANIZATION

INTERNATIONAL CENTRE FOR THEORETICAL PHYSICS
34100 TRIESTE (ITALY) - P.O.B 586 - MIRAMARE - STRADA COSTIERA 11 - TELEPHONE: 2240-1
CABLE: CENTRATOM - TELEX 460392 - I

H4.SMR/204 - 7

WINTER COLLEGE ON

ATOMIC AND MOLECULAR PHYSICS

(9 March - 3 April 1987)

(ANALYTICAL LASER SPECTROSCOPY 1)

Saturation Effects, Saturation Broadening

N. OMENETTO

Joint Research Centre
Ispra (Va), Italy

ICTP
WINTER COLLEGE
ON ATOMIC AND
MOLECULAR PHYSICS

TRIESTE , March 1987

"ANALYTICAL
LASER
SPECTROSCOPY 1"

Lecturer : N. OMENETTO

Joint Research Centre

Ispra (Va) , Italy

III.

☆ Saturation Effects: A Closer Look

☆ Saturation Broadening

Extended Model for Saturation in a Two-Level System

COR A. VAN DIJK, N. OMENETTO,* and J. D. WINEFORDNER†
Department of Chemistry, University of Florida, Gainesville, Florida 32611

A model is presented, based on rate equations for a two-level system, which describes both the temporal and time-integrated dependence of the fluorescence signal due to saturation by a broad band and spatially homogeneous laser beam in an optically thin medium. In particular, we discuss the processing of the fluorescence signal by a gated integrator and relations between gate width, laser pulse length, and decay rate constant of the two-level system. It is shown that, even in the relatively simple case of a fully saturating, rectangular laser pulse, the integrated signal is still dependent on atomic and collisional parameters. On the other hand, this dependency can be used to measure these parameters. The only case in which the integrated signal becomes independent of these parameters is the case of a perfectly rectangular portion being sliced out of the time dependent fluorescence signal. An experimental method, which is expected to result in a better approximation of the saturation parameter in the case of the integrated signals, is suggested.

Index Headings: Time-dependent saturation; Fluorescence; Gated integration.

Received 9 January 1981; revision received 27 March 1981.

* Present address: CCR, European Community Center, Stabilimento di Ispra, Analytical Chemistry Division, Bat. 29, 21020 Ispra (Varese), Italy.

† Author to whom correspondence should be addressed.

INTRODUCTION

In recent years, several attempts have been made to measure fluorescence saturation curves, with varying degrees of success.[1-7] It was soon realized by some authors that the simple model based on the steady-state two-level system with a broadband laser was often inadequate to describe experimental situations. Explanations for the failure of the latter model were sought in coherent phenomena,[2] spatial inhomogeneity of the laser beam,[6] temporal variations of the laser pulse,[1,9] and ionization of the excited species.[3,10]

In the present work, we carry the study of saturation in a two-level system a step further. In particular, we will

investigate the effect of an integration over a specified time segment of the fluorescence pulse on the saturation curve. The analysis is started by deriving a general expression for the time dependence of a two-level system, assuming that the rate equation approach is valid. The expression will be valid for arbitrary temporal laser pulse shape. Next, we generate several special cases, taking both simplified and realistic temporal laser pulse shapes. To simulate experimental conditions, we put a boxcar function on the expressions and compare the results with the idealized steady-state case.

I. GENERAL

A two-level model, as depicted in Fig. 1, will be used. The two levels are coupled by a laser field with a time-dependent spectral irradiance $u(t)$, (J m^{-3} Hz^{-1}) whose spectral profile varies little across the atomic line profile. We will also assume that the laser beam is spatially uniform over the region of interest. The case where either one or both of the above assumptions are not justified has been treated by Omenetto *et al.*[11] The medium is taken to be optically thin.

The probability for absorption of a photon per unit of time is then given by $B_{12}u(t)$ (s^{-1}), where B_{12} is the Einstein coefficient for absorption (J^{-1} m^3 s^{-1} Hz). Similarly, $B_{21}u(t)$ (s^{-1}) is the probability for stimulated emission per unit time. We will allow both levels to be degenerate, with degeneracies g_1 and g_2 for level 1 and level 2, respectively; we assume that the (collisional) mixing between the degenerate sublevels is faster than any other time constant occurring in the system. Relations between the various quantities are given by:[12]

$$\frac{B_{21}}{B_{12}} = \frac{g_1}{g_2}, \qquad \frac{A_{21}}{B_{21}} = \frac{8\pi h\nu^3}{c^3}, \tag{1}$$

where c, h, and ν have their usual meanings.

Collisions transferring populations from level 2 to level 1 are represented by the collisional rate constant k_{21}(s^{-1}). Because of the large endoergicity involved, we will neglect k_{12}. The populations of the upper and lower level are represented by $n_2(t)$ and $n_1(t)$, respectively, in units of m^{-3}. Neglecting chemical reactions, ionization, and drain of population to other levels, we will assume that the total population is constant and denote its magnitude by n_T. With these notations, the rate equations can be written as:

$$\left.\begin{aligned}\frac{dn_2(t)}{dt} &= B_{12}u(t)n_1(t) \\ &\quad - [B_{21}u(t) + A_{21} + k_{21}]n_2(t) \\ \frac{dn_1(t)}{dt} &= -B_{12}u(t)n_1(t) \\ &\quad + [B_{21}u(t) + A_{21} + k_{21}]n_2(t) \\ n_1(t) + n_2(t) &= n_T\end{aligned}\right\} \tag{2}$$

The second of these equations is superfluous and the system can be reduced to a single linear differential equation of the first order with time-dependent coefficients

$$\frac{dn_2(t)}{dt} + [B_{12}(1 + g_1/g_2)u(t) + A_{21} + k_{21}]n_2(t) - B_{12}n_T u(t) = 0 \tag{3}$$

As can be verified by differentiation, the solution to this equation is

$$\begin{aligned}n_2(t) = \exp\Big\{-\int_0^t [B_{12}(1 + g_1/g_2)u(t') + A_{21} + k_{21}]dt'\Big\} \times \Big\{K + B_{12}n_T\int_0^t u(t') \\ \cdot\exp\Big[\int_0^{t'} (B_{12}(1 + g_1/g_2)u(t'') + A_{12} + k_{12})dt''\Big]dt'\Big\}\end{aligned} \tag{4}$$

or

$$\begin{aligned}n_2(t) = \exp\Big\{-\int_0^t [g\rho(t') + A]dt'\Big\} \\ \times \Big\{K + n_T\int_0^t \rho(t')\exp\Big[\int_0^{t'} (g\rho(t'') + A)dt''\Big]dt'\Big\}\end{aligned} \tag{5}$$

where K is integration constant (m^{-3}); $\rho(t) = B_{12}u(t)$ (s^{-1}); $g = 1 + g_1/g_2$; and $A = A_{21} + k_{21}$ (s^{-1}).

Several things are worthwhile to note at this point. Firstly, when $\rho(t) = 0$, the upper state population decays exponentially with a time constant A^{-1}; this can also be seen directly from the differential Eq. (3). Secondly, whenever $g\rho(t)$ is larger than $A_{21} + k_{21}$, the temporal behavior is dominated by exponentials whose arguments contain time integrals over the spectral irradiance $u(t)$; this behavior is consequently not necessarily "exponential" in the simple sense of the word.

In the numerical calculations that follow, we will use normalized units, such that $n_T = 1$ and $A_{21} + k_{21} = 1$; thus, all number densities, rate constants, times, and pulse durations are being measured relative to the number 1. In a practical case, say an alkali atom as a trace

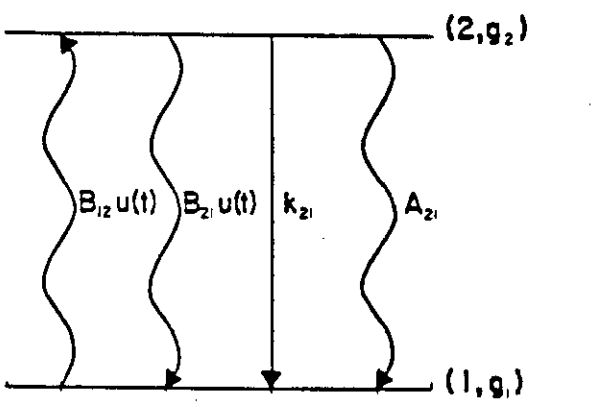

FIG. 1. Level diagram used. Two levels with degeneracies g_1 and g_2 are coupled by induced absorption $B_{12}u(t)$, stimulated emission $B_{21}u(t)$, collisional deexcitation k_{21}, and spontaneous emission A_{21}.

element in an atmospheric pressure flame, n_T could be of the order of 10^{10} cm^{-3}, and $(A_{21} + k_{21})^{-1}$ would be of the order of a few nanoseconds.

A. Special Cases

1. $\rho(t)$ = unit step function

$$\rho(t) = \begin{cases} 0, & t < 0 \\ \rho_0, & 0 \le t. \end{cases} \tag{6}$$

This case is relevant for cw lasers and for pulsed lasers with a long pulse length. Obviously, the rise time of the step function is assumed to be much smaller than any time constant in the two-level system. Substituting Eq. (6) into Eq. (5) and evaluating the various integrals

$$\int_0^t (g\rho_0 + A)dt' = (g\rho_0 + A)t,$$

$$n_T \int_0^t \rho(t')\exp\left[\int_0^{t'} (g\rho(t'') + A)dt''\right]dt'$$

$$= \frac{\rho_0 n_T}{g\rho_0 + A}[-1 + \exp(g\rho_0 + A)t].$$

Applying the initial condition $n_2(0) = 0$ results in

$$n_2(t) = \frac{\rho_0 n_T}{g\rho_0 + A}\{1 - \exp[-(g\rho_0 + A)t]\} \tag{7}$$

Equations analogous to Eq. (7) have been derived by several authors[9, 13-15] for similar systems. We will carry the analysis one step further and investigate how a gating operation, applied to the detected fluorescence signal, affects the results. To this end, we multiply $n_2(t)$ by the boxcar function

$$b(t) = \begin{cases} 1, & t_1 \le t \le t_2 \\ 0, & \text{elsewhere,} \end{cases} \tag{8}$$

It should be noted that the boxcar function is idealized. In a practical case, $b(t)$ will have nonzero rise and decay times. Moreover, integrating with a boxcar is usually accompanied by some amplification; since our main interest is in the relative shapes of the signals and saturation curves, we will assume that the amplification is equal to 1. On the other hand, every detection device has nonzero response times and therefore will integrate the signal to some extent; the discussion will therefore have some relevance even for those cases where a boxcar is not used.

Integrating $b(t)n_2(t)$ over time

$$\int_{t_1}^{t_2} n_2(t)dt = \frac{\rho_0 n_T}{g\rho_0 + A} \times \left\{t_2 - t_1 + \frac{1}{g\rho_0 + A}\right.$$

$$\left.\cdot[\exp(-(g\rho_0 + A)t_2) - \exp(-(g\rho_0 + A)t_1)]\right\}. \tag{9}$$

This result shows that the integrated signal is not simply proportional to the gate width, $t_2 - t_1$, but contains additional dependencies on t_2 and t_1. Saturation curves calculated from Eq. (9) are drawn in Fig. 2 on double logarithmic scales for $t_1 = 0$ and various values of t_2. All of these curves show an initial asymptote with slope +1 and a limiting asymptote with slope 0. The shift in the vertical asymptote between the various curves is due to the term $t_2 - t_1$ in the parentheses of Eq. (9). The most striking feature, however, is the trajectory of the apparent saturation parameter, as indicated by the dashed curve. For the range of $t_2 - t_1$ shown, this parameter ranges from a value of 2 when $t_2 = 0.5$, to a value of 0.5, the latter value being the true saturation parameter as derived from the limiting case, when $t_2 \gg (g\rho_0 + A)^{-1}$:

$$\int_{t_1}^{t_2} n_2(t)dt = \frac{\rho_0 n_T(t_2 - t_1)}{g\rho_0 + A} \tag{10}$$

We will refer to the saturation curve obtained from this limiting case as the curve of stationary population ("cosp"). Note that Eq. (10) agrees with the results obtained for the nonintegrated steady-state case.[13, 16] For low values of the spectral irradiance, the signal is proportional to ρ_0, whereas for large values of ρ_0 Eq. (10) converges to

$$n_T(t_2 - t_1)/g \tag{11}$$

and is thus independent of any rate constant. The remaining proportionality on the total number density and the gate width offers the possibility of decreasing the number density while keeping the integrated signal constant, by simply increasing the gate width, provided, of course, that the signal is constant across the gate.

2. $\rho(t)$ = rectangular pulse

$$\rho(t) = \begin{cases} \rho_0 & 0 \le t \le T \\ 0, & \text{elsewhere.} \end{cases} \tag{12}$$

This choice of $\rho(t)$ approximates experimental situations where pulsed lasers are used. As in the previous case, we assume that the rise and fall time of $\rho(t)$ are faster than any time constant in the two-level system. A more realistic approximation will be presented in case 3. Evaluating the various integrals in Eq. (5), using Eq. (12)

$$\int_0^t [g\rho(t) + A]dt' = \begin{cases} (g\rho_0 + A)t, & t < T \\ At, & T < t \end{cases}$$

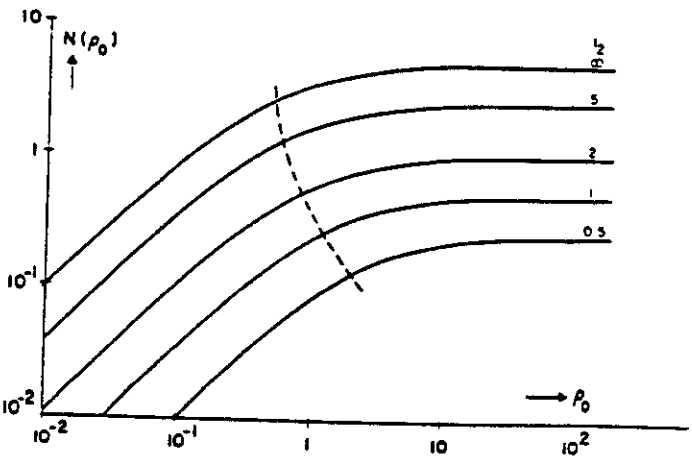

FIG. 2. Saturation curves according to Eq. (9); $n_T = 1$, $A = 1$, $g = 2$, $t_1 = 0$, t_2 ranges from 0.5 (lower curve) to a value much in excess of $(g\rho_0 + A)^{-1}$ (upper curve). The latter curve yields the true value of the saturation parameters, i.e., 0.5. Dashed line: trajectory of the apparent saturation parameter.

and

$$n_T \int_0^t \rho(t')\exp\int_0^{t'} [g\rho(t'') + A]dt''\,dt'$$

$$= \begin{cases} \dfrac{\rho_0 n_T}{g\rho_0 + A}\exp(g\rho_0 + A)t, & t > T \\ 0, & T < t \end{cases}$$

The integration constant K is determined by the condition that at $t = T$ the values of both parts of the solution should be equal, which gives

$$K = \frac{\rho_0 n_T}{g\rho_0 + A}[\exp(AT) - \exp(-g\rho_0 T)]$$

Finally, we obtain

$$n_2(t) = \begin{cases} \dfrac{\rho_0 n_T}{g\rho_0 + A}\{1 - \exp[-(g\rho_0 + A)t]\}, & t < T \\ \dfrac{\rho_0 n_T}{g\rho_0 + A}\{\exp(AT) \\ \quad - \exp[-(g\rho_0 T)]\}\exp(-At), & T < t \end{cases} \tag{13}$$

A plot of $n_2(t)$ vs t is shown in Fig. 3, for various values of ρ_0. Note that, although the laser pulse is rectangular, the ensuing fluorescence pulse has nonzero rise and fall times. In the region $t < T$, $n_2(t)$ is increasing with a time constant involving the probability for induced absorption ρ_0, thus reflecting the pumping action by the laser. Provided that T is sufficiently large compared to the rise time $(g\rho_0 + A)^{-1}$, the steady-state value $\rho_0 n_T/(g\rho_0 + A)$ will be closely approximated during the time that the laser is on. For $t > T$, the excited state population decays solely due to spontaneous emission and quenching collisions. We next consider the effect of integrating $n_2(t)$, as given by Eq. (13) over all time

$$N(\rho_0) \equiv \int_0^\infty n_2(t)dt = \int_0^T n_2(t) + \int_T^\infty n_2(t)dt$$

$$= \frac{\rho_0 n_T}{g\rho_0 + A}\left\{T + [1 - \exp(-(g\rho_0 + A)T)]\right. \tag{14}$$

$$\left.\cdot\left[\frac{1}{A} - \frac{1}{g\rho_0 + A}\right]\right\}$$

From this equation, it is immediately obvious that in general the time-integrated signal is not simply proportional to $\rho_0 n_T/(g\rho_0 + A)$, but contains additional terms involving ρ_0. The latter terms arise because the rise and decay time constants of the excited state population differ from each other and therefore do not compensate for each other when the integral is taken over all time; this can be seen from the second factor in square brackets on the right-hand side of Eq. (14). The effect of the additional ρ_0-containing terms can be seen from Fig. 4, where we have calculated several saturation curves for various values of T. The saturation curves calculated from the full Eq. (14) are seen to have smaller values than those calculated from

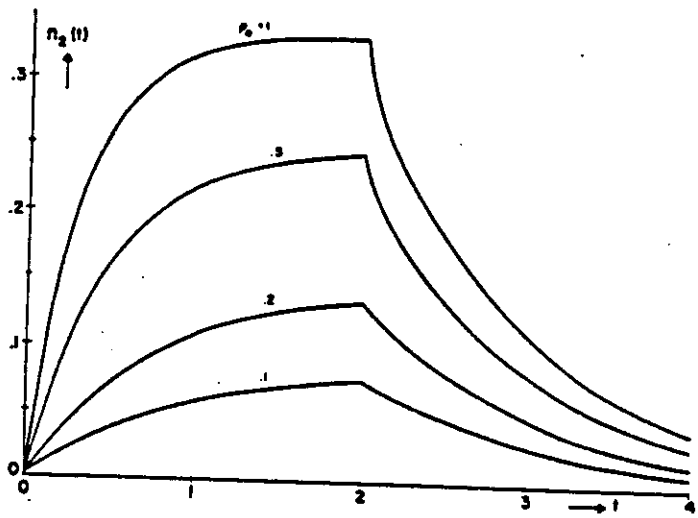

FIG. 3. Fluorescence pulse shapes according to Eq. (13); $n_T = 1$, $A = 1$, $g = 2$. The (rectangular) laser pulse has a duration of $T = 2$ units, and the value ρ_0 of the spectral irradiance is given alongside each curve.

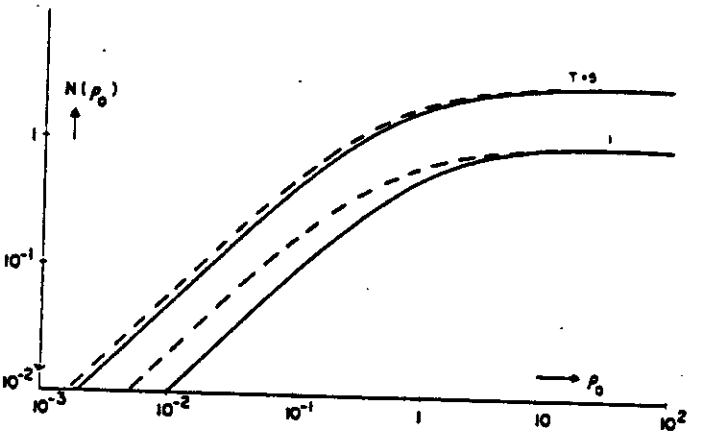

FIG. 4. Saturation curves according to Eqs. (14) (solid curves), and (15) (dashed curves). $n_T = 1$, $A = 1$, $g = 2$. The value of the laser pulse duration is given alongside each pair of curves.

$$N'(\rho_0) \equiv \rho_0 n_T(T + 1/A)/(g\rho_0 + A); \tag{15}$$

the latter equation being the limiting case of Eq. (14) when ρ_0-containing terms in the square brackets are neglected. The fact that $N(\rho_0)$ will be smaller than $N'(\rho_0)$ for every ρ_0, irrespective of A and T can also be inferred directly from Eq. (14), since ρ_0-containing terms have a negative sign and therefore tend to diminish the value of $N(\rho_0)$ with respect to that of $N'(\rho_0)$. The difference in behavior between $N(\rho_0)$ and $N'(\rho_0)$ is important when saturation spectral densities are determined from these curves. According to Omenetto *et al.*,[13] the saturation spectral density is that value of the spectral density which produces a steady-state value of the excited state population which is 50% of the steady-state saturation value. When this definition is applied to both $N(\rho_0)$ and $N'(\rho_0)$ in Fig. 4, it is obvious that the curves relating to $N(\rho_0)$ give higher values for the saturation spectral density than the curves relating to $N'(\rho_0)$. This difference arises because the definition of the above authors applies strictly to Eq. (15), but not to Eq. (14), for which no general explicit expression for the saturation spectral density can be given, due to the transcendental character

of Eq. (14) with respect to ρ_0; consequently, one has to solve Eq. (14) numerically to get the apparent saturation spectral density. Experimental curves derived from integrated signals might behave more like $N(\rho_0)$ than like $N'(\rho_0)$ and this might partly account for some of the too high values of the saturation spectral energy density that have been reported.[1,7]

Because

$$\lim_{\rho_0 \gg A} \frac{\rho_0 n_T}{g\rho_0 + A} \left\{ T + 1[1 - \exp(-(g\rho_0 + A)T)] \cdot \left[\frac{1}{A} - \frac{1}{g\rho_0 + A} \right] \right\} = \frac{n_T}{g} \left(T + \frac{1}{A} \right), \tag{16}$$

both expressions (14) and (15) have the same asymptotic value when the induced absorption dominates the spontaneous emission and quenching. Note that this value still depends on the rate constant of the latter processes, contrary to what would be obtained from the steady-state values of the nonintegrated population density as given by Eq. (13), which is simply n_T/g, as noted by various authors.[9,13] As can be seen from Eq. (16) the influence of the decay on the value of the integrated population density is negligible when the pulse duration T is much larger than $1/A$. When, however, T and $1/A$ are comparable, the integrated, saturated value of n_2, as given by Eq. (15), will depend on the decay constant A. In an experimental situation, this means that the signal is dependent on the composition of the perturber bath, and fluctuations in the signal might be due to fluctuations in this composition. This might explain why integrated fluorescence signals are still noisy, despite the fact that the transition is fully saturated; another noise source is, of course, the total density n_T appearing in Eq. (16), as this quantity often depends critically on temperature.[17] On the other hand, deliberately changing the perturber bath composition might enable one to study the dependence of the integrated and saturated signal on this composition according to Eq. (16), and eventually measure the decay constant A. Another way to achieve the same goal would be to plot the integrated and saturated fluorescence signal in absolute units vs total concentration of seed atoms n_T and derive $T + 1/A$ from the slope of the plot.

In the remainder of this section, we will treat the case where an arbitrary portion is sliced from the pulse as given by Eq. (13). The results obtained will clearly depend on whether the slice is taken before $t = T$, around $t = T$, or after $t = T$. We will briefly discuss each of these cases. The slicing is accomplished by using the boxcar function (8).

a. $t_2 < T$. In this case, one obtains exactly the same solution as found for the case of a step function i.e., Eq. (9), and the discussion pertaining to that equation applies. It should be emphasized, that in the case of $\rho_0 \gg A$, Eq. (9) behaves like $n_T(t_2 - t_1)/g$ and does not involve decay constants as found in Eq. (16). The reason for this is that one slices a rectangular portion out of a quasi-continuum signal and therefore only the time constants of the signal-processing electronics should be important; since we have taken these constants to be 0, the signal is independent of any time constant.

b. $t_1 > T$. This case involves a slice of the decaying part of the excited state population

$$\int_{t_1}^{t_2} n_2(t)\,dt = \frac{\rho_0 n_T}{g\rho_0 + A} (\exp(AT) - \exp(-g\rho_0 T)) \int_{t_1}^{t_2} \exp(-At)\,dt$$

or

$$N(\rho_0) = \frac{\rho_0 n_T}{(g\rho_0 + A)A} (\exp(AT) - \exp(-g\rho_0 T)) (\exp(-At_1) - \exp(-At_2)) \tag{17}$$

Here again, we observe that the signal contains terms in ρ_0, in addition to those contained in $\rho_0 n_T/(g\rho_0 + A)$; these terms will cause the saturation curve corresponding to Eq. (17) to deviate from the simple behavior predicted by $\rho_0 n_T/(g\rho_0 + A)$, in the region where $g\rho_0 T \approx 1$.

Whenever the pulse duration exceeds appreciably the induced life time of the ground state ρ_0^{-1}, the simple behavior of $\rho_0 n_T/(g\rho_0 + A)$ is recovered. This is because the amplitude of the sliced portion is still proportional to the amplitude of the portion of the pulse with the laser on. Since the amplitude of the latter portion at $t = T$ is proportional to $\rho_0 n_T/(g\rho_0 + A)$ and the factor within the first parentheses on the right-hand side of Eq. (17), the amplitude of the sliced portion also depends on these factors. To obtain the limiting case of high spectral irradiance, we require: $g\rho_0 \gg A$ and $g\rho_0 \gg 1/T$, in which case we get

$$N = n_T[\exp(-A(t_1 - T)) - \exp(-A(t_2 - T))]/gA \tag{18}$$

This expression contains the decay constant A, which is only to be expected, since we are taking a portion of the decaying part of the excited state population. However, in the limit of both $t_1 - T$ and $t_2 - T \ll 1/A$, the expression becomes independent of A and depends solely on the total number density, the gate width, and the degeneracy of the levels

$$N \approx n_T(t_2 - t_1)/g, \tag{19}$$

which is identical to the results found for the case of a saturating, quasi-continuum laser pulse [Eq. (11)].

Note that the requirement $g\rho_0 \gg 1/T$, leading to Eq. (18), might be harder to meet for shorter laser pulses.

c. $t_1 < T < t_2$. Here we have to take integrals over both the part of the expression (13) valid for $t < T$ and the part valid for $T < t$:

$$\int_{t_1}^{t_2} n_2(t)\,dt = \frac{\rho_0 n_T}{g\rho_0 + A} \cdot \int_{t_1}^{T} \{1 - \exp[-(g\rho_0 + A)t]\}\,dt + \frac{\rho_0 n_T}{g\rho_0 + A} \cdot [\exp(AT) - \exp(-g\rho_0 T)] \int_{T}^{t_2} \exp(-At)\,dt$$

which gives

$$N(\rho_0) = \frac{\rho_0 n_T}{g\rho_0 + A}\left\{T - t_1 + \frac{1}{g\rho_0 + A}\cdot[\exp(-(g\rho_0 + A)T) - \exp(-(g\rho_0 + A)t_1)]\right\} + \frac{\rho_0 n_T}{(g\rho_0 + A)A}[\exp(AT) - \exp(-g\rho_0 T)]\,[\exp(-AT) - \exp(-At_2)], \tag{20}$$

a result which can also be obtained by replacing t_2 by T in Eq. (9), t_1 by T in Eq. (17), and then adding both equations. Eq. (20) combines aspects of the two previous cases; $t_2 > T$ and $t_1 < T$, and therefore needs little elaboration. It is obvious that the dependence on the radiatively induced absorption probability ρ_0 is even more complicated than in either one of the two previous cases. In the limit of $\rho_0 \gg A$, we get

$$N = \frac{n_T}{g}\{T - t_1 + [1 - \exp(-A(t_2 - T))]/A\} \tag{21}$$

which reduces to

$$N = n_T(t_2 - t_1)/g \tag{22}$$

when $t_2 - T \ll 1/A$; this means that we close the gate before any appreciable decay of the excited state population has taken place. Because of the fast rise time induced by the saturating laser pulse, a steady-state population is achieved for every $t < T$ and therefore the moment of opening the gate is irrelevant, provided $t_1 < T$.

Eq. (22) is proportional to the familiar result obtained for the steady-state nonintegrated excited state population density.

3. In the two previous cases, we dealt with rather idealized laser pulse shapes. In this section, we will consider the effect of a laser pulse having nonzero rise and fall times.

A convenient function to represent a temporal laser shape is

$$\rho(t) = P(t/T)\exp(-t/T) \tag{23}$$

where P is the time-independent amplitude of the spectral irradiance. The maximum of $\rho(t)$ occurs at $t = T$ and has the value P/e. For $t \ll T$, the spectral irradiance increases linearly with t. Rise time t_r and fall time t_f can be obtained by solving (numerically): $(t_r/T)\exp(-t_r/T) = (1 - e^{-1})/e$, respectively, $(t_f/T)\exp(-t_f/T) = e^{-2}$. Similarly, the full width at half-maximum follows from subtracting t_2 and t_1, where t_1 and t_2 are solutions of $(t_{1,2}/T)\exp(-t_{1,2}/T) = 1/(2e)$.

The pulse shape as given by Eq. (23) does not allow an analytical solution of Eq. (5) and we therefore resort to numerical solutions. Rather than substituting $\rho(t)$ from Eq. (23) into the general solution (4), we will solve the differential Eq. (3) directly, as this turns out to be more efficient computationally. We used the Runga-Kutta method to solve Eq. (3) and obtain the upper state population $n_2(t)$, shown in Fig. 5b for various values of the peak spectral irradiance P. A plot of the laser pulse shape is also shown in Fig. 5a. For low values of P, the maximum of the excited state population $n_2(t)$ is seen to lag with respect to the peak of the laser pulse, but with increasing P the lag decreases. This decrease in the lag demonstrates the steepening effect of an increase in laser power on the leading edge of $n_2(t)$, similar to that observed in Fig. 3 and also predicted by Omenetto and Winefordner.[13] A slower-than-linear increase in $n_2(t)$, across the profile shown, can be observed with increasing P, thus reflecting the saturation. This sublinear increase is accompanied by a broadening of the pulse shape. The latter broadening has been observed experimentally[4] and can be understood qualitatively when one realizes that, with increasing P, saturation sets in earlier in the pulse and levels off later.

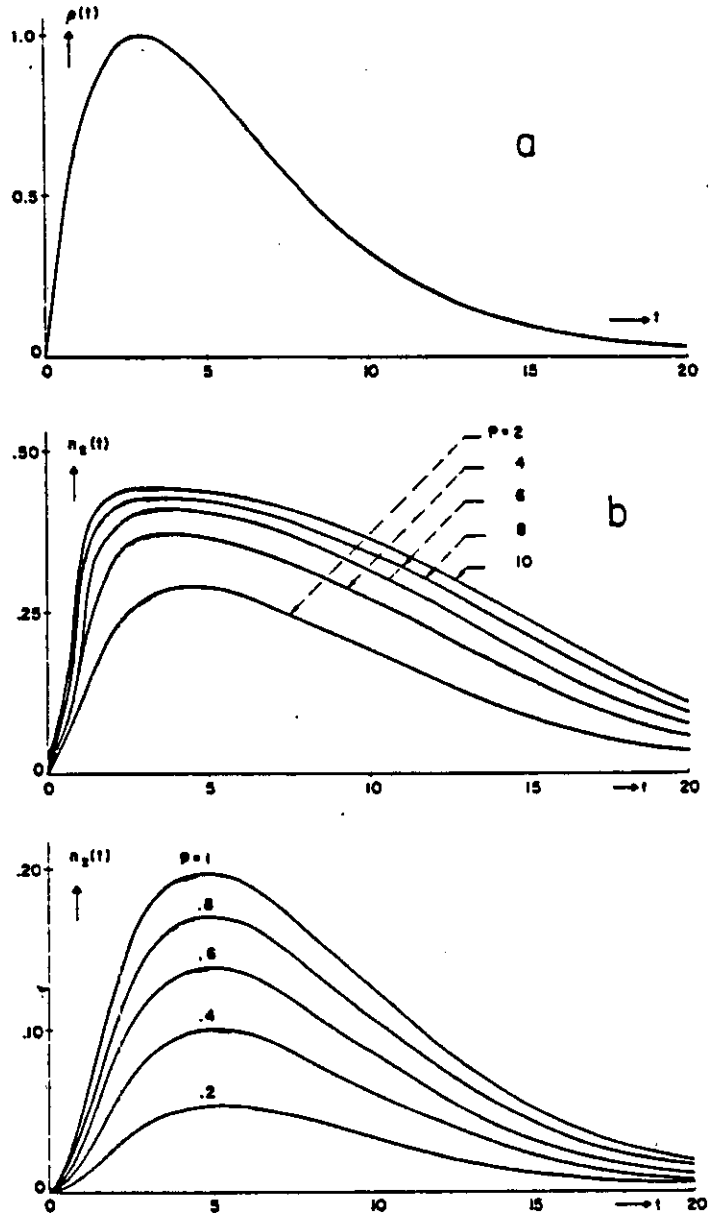

FIG. 5. a. Laser pulse shape according to Eq. (23), with $T = 3$ and $P = 1$. b. Fluorescence pulse shapes obtained by solving numerically Eq. (5) with the laser pulse shape of a, with $n_T = 1$, $A = 1$, $g = 2$. The value of the laser peak irradiance P is given alongside each curve.

Saturation curves on double-log scales, pertaining to the laser shape given by Eq. (23), are shown in Fig. 6.

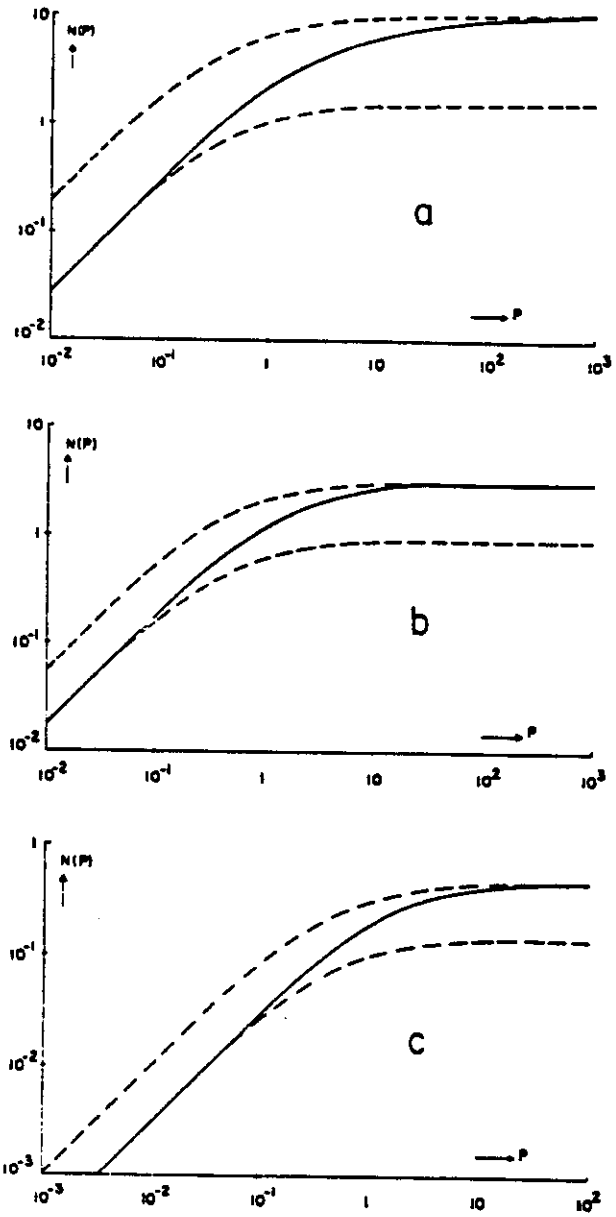

FIG. 6. Saturation curves (solid curves) obtained from numerical integration over an interval $t_2 - t_1$ of numerical solutions to Eq. (5), using Eq. (23) and $n_T = 1$, $A = 1$, $g = 2$, and $T = 3$. The dashed curves are obtained by taking a rectangular slice from a fluorescence pulse with $dn_2/dt = 0$, but otherwise identical parameters. Whence the true saturation parameter $P_s = 0.5$. The apparent saturation parameter P_{as} is found graphically. a. $t_1 = 0$, $t_2 = 20$, $P_{as} = 5.0$; b. $t_1 = 2$, $t_2 = 8$, $P_{as} = 1.7$; c. $t_1 = 2.5$, $t_2 = 3.5$, $P_{as} = 1.5$.

These curves were obtained by numerical integration of $n_2(t)$, as found with the Runga-Kutta algorithm, over a specified time interval, using the trapezoidal rule. Also shown with each saturation curve in Fig. 6 is a pair of saturation curves that would prevail if we had cut a rectangular portion out of a sufficiently long pulse [e.g., the "cosp" of Eq. (10)] with the same value of the parameters. The latter curves have been adjusted using only vertical shifts, such that one of them fits in the low P asymptote (slope = +1), whereas the other fits in the high P asymptote (slope = 0). Integrating practically the whole of $n_2(t)$ over time gives the curve shown in Fig. 6a. Compared to the cosp, the latter curve shows an appreciably slower rate of change with P in the nonlinear region. The apparent saturation parameter (P_{as}) of the curve is larger by a factor of 10 than the saturation parameter of the cosp (P_s). In Fig. 6, we have calculated saturation curves for various slice widths. It can be seen that the curves approach the cosp better for narrower slices, and therefore the discrepancy between the apparent and the true saturation parameters, corresponding to the two types of curves, diminishes. In an actual experimental situation, one has thus to search for a gate width which will bring the curve being measured into perfect overlap with a cosp. Alternatively, one could measure saturation curves using various gate widths centered around the maximum of the fluorescence pulse; then one could plot the apparent saturation parameters found against the gate width and extrapolate to zero width to find the true value of the saturation parameter, provided of course, that no other sources of error, such as spatial or spectral inhomogeneity of the laser beam, occur. The validity of the latter procedure follows from the fact that across a sufficiently narrow slice around the maximum of the fluorescence pulse, $dn_2/dt \simeq 0$ and hence one obtains a cosp.

II. SUMMARY

We have shown that systematic errors occur in the value of the saturation parameters obtained from saturation curves when using a gated integrator to process the fluorescence signal. The magnitude of these errors depends on the characteristics of the laser pulse as well as on the rate constants of the two-level system. Moreover, the width and position of the gate within the fluorescence pulse affects the shape of the saturation curve. Measuring the apparent saturation parameter as a function of the gate width of the integrator and extrapolating to zero gate width is expected to yield the true value of the saturation parameter.

Any saturation curve, derived from a signal containing components that vary with time, will give a too high value for the saturation parameter. This follows from the consideration that saturation is harder to achieve for a faster changing population.

The time-integrated and fully saturated fluorescence signal resulting from a rectangular laser pulse is shown to contain the decay constants of the two-level system in a simple way and therefore is expected to provide a means of measuring these constants.

Throughout the analysis, we have assumed the gate of the integrator to be perfectly rectangular. An attempt to deconvolute the instrumental response and the fluorescence signal has been made by de Olivares[1] for a specific choice of the functions involved and zero gate width.

ACKNOWLEDGMENT

Research was supported by AFOSR-F49620-80C-0005.

1. D. R. de Olivares, Thesis, Indiana University, Bloomington (1976).
2. B. L. Sharp and A. Goldwasser, Spectrochim. Acta 31B, 431 (1976).
3. B. Smith, J. D. Winefordner, and N. Omenetto, J. Appl. Phys. 48, 2676 (1977).
4. R. A. Van Calcar, M. J. M. Van de Ven, B. K. Van Uitert, K. J. Biewenga, Tj. Hollander, and C. Th. J. Alkemade, J. Quant. Spectrosc. Radiat. Transfer 21, 11 (1979).
5. C. A. Van Dijk, P. J. Th. Zeegers, G. Nienhuis, and C. Th. J. Alkemade, J. Quant. Spectrosc. Radiat. Transfer 20, 55 (1978).
6. M. B. Blackburn, J. M. Mermet, G. D. Boutillier, and J. D. Winefordner, Appl. Opt. 18, 1804 (1979).

7. J. M. Salter, D. D. Burgess, and N. A. Ebrahim, J. Phys. B **12**, L759 (1979).
8. J. W. Daily, Appl. Opt. **17**, 225 (1978).
9. D. R. de Olivares and G. M. Hieftje, Spectrochim. Acta **33B**, 79 (1978).
10. C. A. Van Dijk and C. Th. J. Alkemade, Combust. Flame **38**, 37 (1980).
11. N. Omenetto, J. Bower, J. Bradshaw, C. A. Van Dijk, and J. D. Winefordner, J. Quant. Spectrosc. Radiat. Transfer **24**, 147 (1980).
12. A. C. G. Mitchell and M. W. Zemansky, *Resonance Radiation and Excited Atoms* (Cambridge, 1971), Chap. III, p. 94.
13. N. Omenetto and J. D. Winefordner, *Progress in Analytical Atomic Spectroscopy* (Pergamon, New York, 1979), Vol. 2, Chap. I, p. 9.
14. T. Tsai and T. F. Morse, IEEE J. Quantum Electron. QE-15, 1334 (1979).
15. G. Zizak, J. D. Bradshaw, and J. D. Winefordner, Appl. Opt. **19**, 3631 (1980).
16. N. Omenetto, P. Benetti, L. P. Hart, J. D. Winefordner, and C. Th. J. Alkemade, Spectrochim. Acta **28B**, 289 (1973).
17. W. M. Fairbank Jr., T. W. Hänsch, and A. L. Schawlow, J. Opt. Soc. Am. **65**, 199 (1975).

Spectrochimica Acta, Vol. 37B, No. 11, pp. 1009–1014, 1982.
Printed in Great Britain.

0584-8547/82/111009-04$03.00/0

COMMUNICATION

Response time of two- and three-level atomic and molecular systems to steplike excitation

(*Received* 30 *June* 1982)

Terms like systems' *response time, pumping time, radiative* and *collisional lifetime* have been repeatedly used in the literature concerning atomic and molecular fluorescence under laser irradiation[1–9]. We simply wish to present here some considerations that are believed to be useful to elucidate the difference between these terms, which should not be used indiscriminately, and are not always interchangeable.

The discussion which follows is valid for both atomic and molecular systems and with the assumptions usually made, i.e. optically thin vapor, spectrally continuum excitation and no laser-enhanced chemical reactions and/or ionization (which could, however, be incorporated in an additional level). Most importantly, the system does not undergo Rabi oscillations during the response time. As usual, we should stress the fact that the system and the excitation conditions referred to here are highly idealized. However, our aim is merely to point out some fundamental differences in the concepts related to the above mentioned terms and therefore, in this context, the discussion has a more general validity.

Consider an atomic (molecular) system with 3 levels herewith indicated as levels 1, 2 and 3, in order of increasing energy. n_i is the population density of level i (cm^{-3}); g_i is its statistical weight. The total number density, n_T, is equal to $n_1 + n_2 + n_3$. The collisional constants considered here are k_{31}, k_{32} and k_{21} since k_{12}, k_{13} and k_{23} are assumed to be negligible. A_{31} and A_{32} are the spontaneous radiative rate constants (s^{-1}) while $\rho_\nu(\nu)\,B_{13}$ and $\rho_\nu(\nu)\,B_{31}$ are the induced radiative rate constants (s^{-1}). $\rho_\nu(\nu)$ is the laser spectral energy density ($J\,cm^{-3}\,Hz^{-1}$). For molecules, A_{32} is zero and one should consider A_{21} for the phosphorescence process. In this case, k_{32} is the intersystem crossing rate.

The following definitions and relationships hold:

$(n_3^{ss})_{2L}^{sat}$ = steady state (ss) population density (cm^{-3}) of level 3 at saturation (superscript "sat") in *absence* of level 2 (2L stands for two-level system)

$(n_3^{ss})_{2L}^{sat} = n_T B_{13} \rho_{13}(\nu)(t_r)_{2L}$;

$(n_3^{ss})_{3L}^{sat}$ = steady state (ss) population density (cm^{-3}) of level 3 at saturation (superscript "sat") in *presence* of level 2 (3L stands for three-level system)

$(n_3^{ss})_{3L}^{sat} = n_T B_{13} \rho_{13}(\nu)(t_r)_{3L}$;

τ = lifetime of level 3 for a two-level system, defined as the average time spent

[1] R. M. Measures, *J. Appl. Phys.* **39**, 5232 (1968).
[2] N. Omenetto and J. D. Winefordner, *Prog. Anal. Atom. Spectrosc.* **2**(12), 1 (1979).
[3] R. M. Measures and P. G. Cardinal, *Phys. Rev. A* **23**, 804 (1981).
[4] M. Mailänder, *J. Appl. Phys.* **49**, 1256 (1978).
[5] D. R. de Olivares and G. M. Hieftje, *Spectrochim. Acta* **33B**, 79 (1978); *Spectrochim Acta* **36B**, 1059 (1981).
[6] D. H. Campbell and J. W. L. Lewis, *Appl. Optics* **20**, 4102 (1981).
[7] D. Stepowski and M. J. Cottereau, *Appl. Optics* **18**, 354 (1979).
[8] R. P. Lucht, Ph.D. Thesis, School of Mechanical Engineering, Purdue University, West Lafayette, Indiana, U.S.A.
[9] G. D. Boutilier, N. Omenetto and J. D. Winefordner, *Appl. Optics* **19**, 1838 (1980).

by the atom in level 3 before leaving it (by emission of radiation, collision or reaction) in absence of an external excitation fie d;

$\tau = (A_{31} + k_{31})^{-1}$, (s);

$\tau_{rad} = (A_{31})^{-1}$, radiative lifetime of level 3 for a two-level system (s);

$\tau_{col} = (k_{31})^{-1}$, collisional lifetime of level 3 for a two-level system (s). Note that $\tau^{-1} = \tau_{rad}^{-1} + \tau_{col}^{-1}$. Note also that $\tau = \tau_{rad} \cdot Y_{31}$, where $Y_{31} = A_{31}/(A_{31} + k_{31})$ is the quantum efficiency of the transition;

τ' = lifetime of level 3 for a three-level system, (s), defined as above for τ;

$\tau' = (A_{31} + k_{31} + A_{32} + k_{32})^{-1}$;

$\tau'_{rad} = (A_{31} + A_{32})^{-1}$: radiative lifetime of level 3 for the three-level system considered (s);

$\tau_{col} = (k_{31} + k_{32})^{-1}$: collisional lifetime of level 3 for the three-level system considered (s);

t_p = laser pumping time (s), denoting the average time needed for an atom to be transferred from a specific lower to a specific upper level by absorption of a resonant photon from the continuum source; this should by no means be identified with the laser pulse duration;

$$t_p = \left[\left(1 + \frac{g_1}{g_3}\right) B_{13}\rho_{13}(\nu)\right]^{-1};$$

$(t_r)_{2L}$ = response time of the population of level 3 for a two-level system, (s), denoting the time needed for n_3 to reach a specified fraction of its final value when the atoms are exposed to a steplike excitation function; in this case, one could also speak of the "response time of the system";

$$(t_r)_{2L} = \left[\left(1 + \frac{g_1}{g_3}\right) B_{13}\rho_{13}(\nu) + A_{31} + k_{31}\right]^{-1};$$

$(t_r)_{3L}$ = response time of the population of level 3 for the three-level system considered (s), defined as above for $(t_r)_{2L}$;

$$(t_r)_{3L} = \left[B_{13}\rho_{13}(\nu)\left(\frac{k_{32} + A_{32}}{k_{21}}\right) + B_{13}\rho_{13}(\nu) \times \left(1 + \frac{g_1}{g_3}\right) + A_{31} + k_{31} + A_{32} + k_{32}\right]^{-1}$$

From the above nomenclature, we obtain

$$(t_r)_{2L} = \frac{t_p\tau}{t_p + \tau} \tag{1}$$

and

$$(t_r)_{3L} = \frac{t_p\tau'}{\tau'\left(1 + \frac{K}{G}\right) + t_p} \tag{2}$$

where

$$K \equiv \left(\frac{A_{32} + k_{32}}{k_{21}}\right) \quad \text{and} \quad G \equiv \left(1 + \frac{g_1}{g_3}\right).$$

Ratioing Eqns (1) and (2), gives

$$\frac{(t_r)_{3L}}{(t_r)_{2L}} = \left(\frac{\tau'}{\tau}\right)\left[\frac{t_p + \tau}{t_p + \tau'\left(1 + \frac{K}{G}\right)}\right]. \tag{3}$$

Equation (3) shows the difference in the response time of the level reached by the laser for the 2- and 3-level schemes considered as a function of the parameters under discussion, i.e., lifetime and pumping time. This equation can now be discussed for the two cases of interest, namely for linear interaction between the radiation and the absorbing system and for saturation conditions.

Case 1: *Linear interaction*

Linear interaction means that

$$\tau \quad \text{and} \quad \tau' \ll t_p \tag{4a}$$

and therefore

$$\frac{(t_r)_{3L}}{(t_r)_{2L}} = \left[\frac{t_p}{t_p + \tau'[1 + (K/G)]}\right]\left(\frac{\tau'}{\tau}\right). \tag{4b}$$

Case 1.1. Fast collisional coupling between levels 2 and 1. This implies that

$$\frac{K}{G} \ll 1 \quad \text{or} \quad k_{21} \gg (k_{32} + A_{32}). \tag{5a}$$

Then, we also have

$$\tau'\left(1 + \frac{K}{G}\right) \ll t_p \tag{5b}$$

and therefore, as one would have expected

$$\frac{(t_r)_{3L}}{(t_r)_{2L}} = \frac{\tau'}{\tau}. \tag{6}$$

Case 1.2. Level 2 is acting as a sink because of its low collisional coupling with level 1. This implies that

$$\frac{K}{G} \gg 1 \quad \text{or} \quad k_{21} \ll (A_{32} + k_{32}). \tag{7a}$$

Then, we also have

$$\frac{(t_r)_{3L}}{(t_r)_{2L}} = \left(\frac{\tau'}{\tau}\right)\left[\frac{t_p}{t_p + \tau'(K/G)}\right]. \tag{7b}$$

If the second term in the denominator is much less than t_p, then Eqn (6) again results. If the contrary holds, then Eqn (7b) becomes

$$\frac{(t_r)_{3L}}{(t_r)_{2L}} = \frac{t_p G}{\tau K} \tag{8a}$$

or, using the definitions given in the nomenclature,

$$\frac{(t_r)_{3L}}{(t_r)_{2L}} = \left[\frac{k_{21}}{B_{13}\rho_{13}(\nu)}\right]\left[\frac{A_{31} + k_{31}}{A_{32} + k_{32}}\right] \tag{8b}$$

and the ratio is essentially governed by the magnitudes of the collisional downward coupling of level 2 with the ground level and the excitation rate.

Case 2: *Saturation*

At saturation, $t_p \ll \tau, \tau'$. We have again two possibilities:

Case 2.1. Fast coupling, i.e. Eqn (5a) holds. We then have from Eqn (3)

$$(t_r)_{3L} = (t_r)_{2L} \tag{9}$$

which is again the result expected since the 3-level system in this case can be considered as a 2-level system in which levels 1 and 2 have coalesced in a single level.

Case 2.2. Level 2 is acting as a sink, i.e. Eqn (7a) holds. We then have from Eqn (3).

$$\frac{(t_r)_{3L}}{(t_r)_{2L}} = \frac{\tau'}{t_p + \tau'(K/G)} = \frac{G}{K} \tag{10a}$$

or

$$\frac{(t_r)_{3L}}{(t_r)_{2L}} = \left(1 + \frac{g_1}{g_3}\right)\left(\frac{k_{21}}{A_{32} + k_{32}}\right). \tag{10b}$$

In this case, the response time in the 3-level case will be much faster than that of a two-level system, since atoms (molecules) accumulating in level 2 will not be recycled. This has also implications on the value of the *saturation spectral irradiance*, which can be very low compared to that of a 2-level scheme[10–12].

Acknowledgements—The useful comments and discussions with Prof. C. Th.J. Alkemade are gratefully acknowledged.

Joint Research Centre
Chemistry Division
21020 *Ispra (Varese)*
Italy

N. OMENETTO

[10] M. A. BOLSHOV, A. V. ZYBIN, V. G. KOLOSHNIKOV and K. N. KOSHELEV, *Spectrochim. Acta* 32B, 279 (1977).
[11] G. D. BOUTILIER, J. D. WINEFORDNER and N. OMENETTO, *Appl. Optics* 17, 3482 (1978).
[12] N. OMENETTO, C. A. VAN DUK and J. D. WINEFORDNER, *Spectrochim. Acta* 37B, 000 (1982).

Spectrochimica Acta, Vol. 37B, No. 8, pp. 703–711, 1982.
Printed in Great Britain.

0584-8547/82/080703-09$03.00/0
Pergamon Press Ltd.

Some considerations on the saturation parameter for 2- and 3-level systems in laser excited fluorescence

N. OMENETTO*, C. A. VAN DUK and J. D. WINEFORDNER
Department of Chemistry, University of Florida, Gainesville, FL 32611, U.S.A.

(*Received* 12 *January* 1982)

Abstract—The parameter "saturation spectral irradiance", defined for a spectrally continuum laser source interacting in a non-linear manner with a dilute atomic (molecular) vapor, is discussed for both 2 and 3 energy level systems. It is shown that the definition of such parameter is meaningful only when steady state conditions are warranted. For short excitation pulses, although steady state can still be attained when the optical transition is saturated, the saturation parameter cannot be evaluated from the conventional fluorescence saturation curve. Therefore, such a definition loses its meaning even for a simple 2-level system. As a consequence, serious experimental errors can occur. The same conclusions apply to a 3-level system. Several experimental possibilities of evaluating the saturation parameter are discussed. Finally, we show that when a 3-level system is compared with a 2-level system, the value of such parameter depends essentially upon the total coupling rate of the third level with the other levels.

INTRODUCTION

THE SO-CALLED *saturation parameter* enters into any discussion on the saturation behavior of an ensemble of atoms or molecules when the irradiation impinging upon the system grows very high. Several papers[1–10] define such a parameter for both monochromatic and continuum radiation sources, pulsed or continuous wave (CW) operation, and 2 or 3 level atomic and molecular systems. As will be shown later, the saturation parameter can be calculated theoretically and derived experimentally in several ways. Its importance lies indeed in the fact that other essential atomic parameters, such as for example the quantum efficiency of the transition can be directly inferred from it.

Some of the topics discussed in this paper can be found sparse in the literature concerning laser excited fluorescence. We felt that it was useful for the readers to present here these and other considerations in a unified manner with the aim of emphasizing several points which, if overlooked, would make the definition of this parameter meaningless and on the other hand cause significant errors in its experimental evaluation.

GENERAL CONSIDERATIONS

The following discussion applies to a dilute vapor of atoms and/or molecules in flames and plasmas at atmospheric pressure irradiated with a laser whose spectral bandwidth is much larger than the line width of the absorbing species. When the laser source is monochromatic, i.e. when its bandwidth is much narrower than the ab-

[1] R. M. MEASURES, *J. Appl. Phys.* **39**, 5232 (1968).
[2] R. M. MEASURES, N. DREWELL and P. CARDINAL, *J. Appl. Phys.* **50**, 2662 (1979).
[3] N. OMENETTO and J. D. WINEFORDNER, *Prog. Anal Atom. Spectrosc.* **2**, 1 (1979).
[4] E. H. PIEPMEIER, In; *Analytical Laser Spectroscopy* (Edited by N. OMENETTO). Chap. 3. Wiley-Interscience, New York (1979).
[5] D. R. OLIVARES and G. M. HIEFTJE, *Spectrochim. Acta* **33B**, 79 (1978).
[6] N. OMENETTO, J. D. WINEFORDNER and C. TH. J. ALKEMADE, *Spectrochim. Acta* **30B**, 335 (1975).
[7] G. D. BOUTILIER, M. B. BLACKBURN, J. M. MERMET, S. J. WEEKS, H. HARAGUCHI, J. D. WINEFORDNER and N. OMENETTO, *Appl. Optics* **17**, 2291 (1978).
[8] R. A. VAN CALCAR, M. J. M. VAN DEN VEN, B. K. VAN UITERT, K. J. BIEWENGA, TF. HOLLANDER and C. TH. J. ALKEMADE, *J. Quant. Spectrosc. Radiat. Transfer* **21**, 11 (1979).
[9] J. W. DAILY, *Appl. Optics* **17**, 225 (1978).
[10] C. TH. J. ALKEMADE, Plenary lecture given at the 5th ICAS and 20th CSI, Prague 1977.

*Present Address: Joint Research Centre, Analytical Chemistry Division, 21020 Ispra(VA), Italy.

sorption linewidth, then we shall assume that velocity changing collisions in the flame or plasma are very fast so that atoms and molecules will contribute to the absorption over the entire absorption profile. Rate equations are considered to be also valid because of the fast dephasing time associated with these systems at atmospheric pressure. Laser-enhanced chemical reactions and ionization, which are known to occur in flames to a considerable extent [11–14] are disregarded here. This assumption can be partially justified when the laser is pulsed and the pulse duration does not exceed a few nanoseconds, since the rate constants for the above mentioned processes are considered to be on a longer time scale. However, for the present discussion on the saturation parameter, these side reactions can be phenomenologically associated with the third level not directly coupled by the laser radiation (see below). The detection system is assumed to be able to faithfully reproduce the temporal variation of the atomic (molecular) population of the excited state, responding to a spatially homogeneous laser beam, whose temporal shape is assumed to be steplike or rectangular. The conventional boxcar detection scheme and its associated problems have been recently discussed by VAN DIJK *et al.* [15].

When all the above assumptions are met, the *steady state* fluorescence radiance, B_F ($Js^{-1}cm^{-2}sr^{-1}$), plotted vs the laser spectral irradiance, E_ν ($Js^{-1}cm^{-2}Hz^{-1}$), will show a behavior similar to that depicted in Fig. 1. We call these curves the "fluorescence saturation curves". The linear asymptote, describing the interaction at low laser irradiances, is seen to intersect the infinite irradiance asymptote, when saturation of the optical transition is achieved, at a specific irradiance, E'_ν, referred here as the *steady state saturation spectral irradiance.* As shown in Fig. 1, such a parameter is defined as the irradiance producing a steady state value of the excited state population which is 50% of the steady state saturation value. As indicated by WUCHERS, and reported by VAN DIJK [12], E'_ν can be found even if complete saturation is not yet

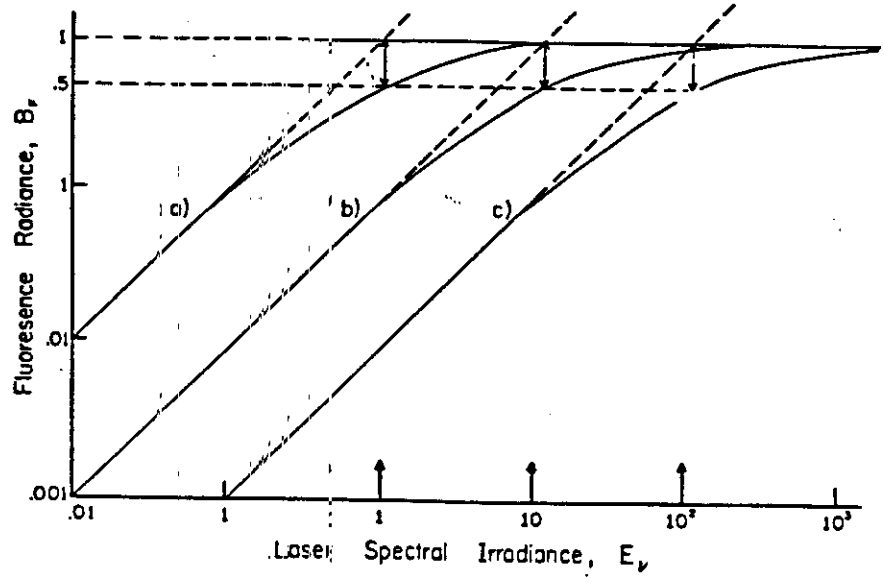

Fig. 1. Steady state fluorescence saturation curves. The arrows drawn on the abscissa correspond to the different saturation parameters obtained according to the definition given in the text for three different values of the quantum efficiency. Curve (a): $Y = 1$; curve (b): $Y = 0.1$; curve (c): $Y = 0.01$.

[11] R. B. GREEN, R. A. KELLER, P. R. SCHENCK, J. C. TRAVIS and G. G. LUTHER, *J. Am. Chem. Soc.* 98, 8517 (1976).
[12] C. A. VAN DIJK, P. J. TH. ZEEGERS, G. NIENHUIS, C. TH. J. ALKEMADE, *J. Quant. Spectrosc. Radiat. Transfer* 20, 55 (1978).
[13] C. H. MULLER, K. SCHOFIELD and M. STEINBERG, *J. Chem. Phys.* 72, 6620 (1980).
[14] D. R. CROSLEY, *Laser Probes for Combustion Chemistry*, ACS Symposium Series No. 134 (1980).
[15] C. A. VAN DIJK, N. OMENETTO and J. D. WINEFORDNER, *Appl. Spectrosc.* 35, 389 (1981).

achieved by noting that it corresponds to the point where the linear asymptote reaches a value which is twice that of the actual fluorescence saturation curve.

The usual experimental means of obtaining the curves of Fig. 1 is to operate the laser at its maximum power while recording the wavelength integrated fluorescence signal, and then decreasing the laser irradiance by inserting into the beam before the flame several calibrated neutral density filters down to the point where linearity exists again between the fluorescence signal and the laser power.

If the above (given) definition of the saturation spectral irradiance is applied to the expressions obtained by solving the steady state rate equations for 2 and 3 level atomic systems for the fluorescence radiance, we obtain the relations given below.

Two-level systems (Fig. 2a)

For this case

$$E_{\nu_{13}}^{s-2L} = \left(\frac{cA_{31}}{B_{31}Y_{31}^{2L}}\right)\left(\frac{g_1}{g_1+g_3}\right). \tag{1}$$

Here, $E_{\nu_{13}}^{s-2L}$ stands for the saturation spectral irradiance pertinent to a two level system, as indicated by the superscript $2L$, c (cm s^{-1}) is the velocity of light, A_{31}(s^{-1}) is the Einstein coefficient of spontaneous emission, Y_{31}^{2L} (dimensionless) is the quantum efficiency of the transition, where $2L$ again appears as superscript and indicates that only two energy levels are considered, and g_1 and g_3 represent the statistical weights of the levels. The quantum efficiency is simply given by

$$Y_{31}^{2L} = \frac{A_{31}}{A_{31}+k_{31}} = \frac{\tau_{eff}}{\tau_{rad}}, \tag{2}$$

where k_{31}(s^{-1}) is the overall collisional quenching rate constant and τ_{eff} and τ_{rad} are the effective and radiative lifetimes (s) of level 3, respectively. The inverse proportionality between the saturation parameter and the quantum efficiency given in Eqn (1)

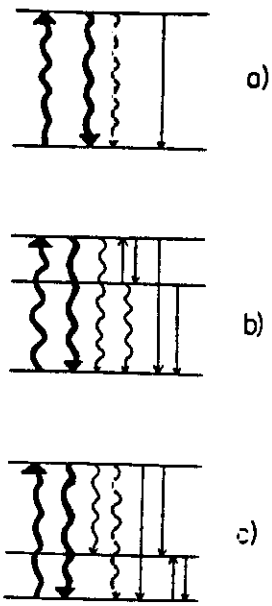

Fig. 2. Schematic energy level diagram for: (a) two energy levels; (b) and (c): three energy level systems. Wavy lines indicate stimulated absorption, stimulated emission and spontaneous emission; straight lines indicate collisional transitions. In case (b), the third level is radiatively connected with the ground state (sodium-type atoms) while in case (c) the third level is radiately coupled with the laser excited level.

and shown in Fig. 1 can be expressed in terms of fundamental constants and the frequency by using the well-known relationship between the Einstein coefficients

$$B_{31} = A_{31}\left(\frac{c^3}{8\pi h\nu^3}\right), \tag{3}$$

where ν (Hz) is the frequency of the transition and h (Js) is the Planck constant. We therefore obtain

$$E^{s-2L}_{\nu_{13}} \equiv \frac{\Phi_l}{\delta\nu_l S_l} = \left(\frac{8\pi h\nu^3}{c^2}\right)\left(\frac{1}{Y^{3L}_{31}}\right)\left(\frac{g_1}{g_1+g_3}\right). \tag{4}$$

In this equation, the laser parameters, such as power Φ_l (Js^{-1}), spectral bandwidth $\delta\nu_l$ (Hz) and geometric cross section S_l (cm^2), are indicated.

Sodium-like three level systems (Fig. 2b)

By this terminology, we refer to a system in which the third level (designated as level 2 in the figure) is radiatively coupled with the ground state but not with the level directly reached by the laser radiation. By solving the steady state rate equation and proceeding as before, we obtain

$$(E^{s-3L}_{\nu_{13}})_{Na} = \left(\frac{g_1}{g_3}\right)\left(\frac{cA_{31}}{B_{31}Y^{3L}_{31}}\right)\left(\frac{1}{1+\dfrac{g_1}{g_3}+\dfrac{k_{32}}{A_{21}+k_{21}+k_{23}}}\right). \tag{5}$$

As one can see, here the collisional rate constants involving the third level enter the definition of the saturation parameter, which therefore is not simply related to the quantum efficiency of the transition as in the case of a 2-level system. This outcome has been clearly pointed out in the literature [7]. The superscript $3L$ is meant here to indicate that the definition of quantum efficiency must now include the third level.

Thallium-like three level systems (Fig. 2c)

By analogy with the previous case, we refer here to systems where the third level is radiatively connected with the level directly reached by the laser radiation and collisionally coupled with the ground state. The saturation parameter is given by

$$(E^{2-3L}_{\nu_{13}})_{Tl} = \left(\frac{g_1}{g_3}\right)\left(\frac{cA_{31}}{B_{31}Y^{3L}_{31}}\right)\left(\frac{1}{1+\dfrac{g_1}{g_3}+\dfrac{A_{32}+k_{32}}{k_{21}}}\right), \tag{6}$$

and similar considerations apply.

The saturation parameter expressions derived (Eqns (1), (5), (6)) allow a comparison to be made of the variation of the saturation spectral irradiance when a third level is added to the two levels coupled by the laser radiation. It is worth repeating here that the third level can also be identified with laser enhanced reactions or ionization occurring within the time scale of the absorption-emission process. When comparing the expressions, Eqn (2) for the quantum efficiency has to be modified accordingly. For sodium-like three level systems, we have [16]

$$(Y^{3L}_{31})_{Na} = \frac{A_{31}}{A_{31}+k_{31}+k_{32}-\dfrac{k_{32}k_{23}}{A_{21}+k_{21}+k_{23}}}, \tag{7}$$

[16] F. R. LIPSETT, The quantum efficiency of luminescence, in *Progress in Dielectrics*, Vol. 7. Icliffe (1968).

and for thallium-like systems

$$(Y_{31}^{3L})_{Tl} = \frac{A_{31}}{A_{31} + A_{32} + k_{31} + k_{32}}. \tag{8}$$

In the sodium case, the influence of the third level on the value of the saturation parameter can therefore be evaluated by the following expression

$$\left(\frac{E_{\nu_{13}}^{s-3L}}{E_{\nu_{13}}^{s-2L}}\right)_{Na} = \left(\frac{g_1 + g_3}{g_3}\right)\left\{1 + \left(\frac{k_{32}}{A_{31} + k_{31}}\right)\left(\frac{A_{21} + k_{21}}{A_{21} + k_{21} + k_{23}}\right)\right\} \times \left\{\frac{1}{(g_1 + g_3)/g_3 + k_{32}/(A_{21} + k_{21} + k_{23})}\right\}. \tag{9}$$

Similarly, for the thallium case, we derive the following expression

$$\left(\frac{E_{\nu_{13}}^{s-3L}}{E_{\nu_{13}}^{s-2L}}\right)_{Tl} = \left(\frac{g_1 + g_3}{g_3}\right)\left\{1 + \frac{A_{32} + k_{32}}{A_{31} + k_{31}}\right\} \times \left\{\frac{1}{(g_1 + g_3)/g_3 + (A_{32} + k_{32})/k_{21}}\right\}. \tag{10}$$

Several conclusions are evident from Eqns (9) and (10), and they are outlined below:

(i) For both systems, the change in the saturation parameter when a third level is included is essentially governed by the collisional coupling of the third level with the other two levels. This is especially true for atmospheric pressure hydrocarbon flames where quenching is severe and therefore radiative disequilibrium is relatively unimportant since the spontaneous radiative rates are much less than the collisional rates;

(ii) for the sodium-like case, substituting the known values of A_{31} and A_{21}, assuming similar quenching constants and making use of the balance relations between k_{32} and k_{23}, one can easily see that $E_{\nu_{13}}^{s-2L}$ and $E_{\nu_{13}}^{s-3L}$ differ by only approximately 10%. This outcome reflects indeed the fact that sodium can be considered as a special two-level system in which the upper excited doublet coalesces into single level whose statistical weight is the sum of the statistical weights of the individual levels [1, 8, 10];

(iii) for the thallium-like case, if we assume that A_{32} and k_{32} do not greatly differ from A_{31} and k_{31}, Eqn (10) is governed by the ratio between the rate constants shown in the last brackets on the right hand side of the equation. Here, we can distinguish two distinct situations. If fast coupling exists between the third level and the ground state ($k_{21} \gg A_{32} + k_{32}$), then the saturation parameter for a 3-level system is *larger* than that for a 2-level system. However, as seems to be the case of thallium [17], if $k_{21} \ll A_{32} + k_{32}$, the third level acts as a sink for the atoms and accumulation will occur there (metastable level). In this case, the following approximate expression results

$$\left(\frac{E_{\nu_{12}}^{2-3L}}{E_{\nu_{13}}^{s-2L}}\right)_{Tl} \simeq 2\left(\frac{g_1 + g_3}{g_1}\right)\left(\frac{k_{21}}{A_{32} + k_{32}}\right), \tag{11}$$

and $E_{\nu_{13}}^{s-3L}$ can therefore be *much less* than $E_{\nu_{13}}^{s-2L}$. This result has already been pointed out in the literature [18, 19].

From these considerations, one can conclude that it is reasonably simple to predict in which direction the two-level saturation parameter will go after the inclusion of a

[17] J. A. Bellisio and P. Davidovits, *J. Chem. Phys.* **53**, 3474 (1970).
[18] G. D. Boutilier, N. Omenetto and J. D. Winefordner, *Appl. Optics* **19**, 1838 (1980).
[19] M. A. Bolshov, A. V. Zybin, V. G. Koloshnikov and K. N. Koshelev, *Spectrochim. Acta* **32B**, 279 (1977).

third level, provided that the kinetics of its excitation-deexcitation pathways are known or can be estimated.

Other experimental methods of evaluating E_s^*

As stated above, the saturation parameter may be directly evaluated from the experimental plot of a fluorescence saturation curve. Here, the laser power must be known (it is the abscissa), and therefore one needs a reliable means of measuring it. As will be shown later, this method is applicable only when steady state conditions are warranted, i.e. when the excited state population does not change during the measurement time.

The saturation parameter can also be derived from an experimental determination of the effective lifetime of the fluorescent level provided that the radiative lifetime of the same level is known. Lifetime determination in atmospheric pressure flames requires very short excitation pulses and fast electronics to retrieve accurately the temporal fluorescence waveform. Conventional quantum efficiency measurements [20, 21] can also lead to the calculation of E_s^* for a two level system (see Eqn 4).

An indirect method of determining experimentally the saturation parameter comes from the measurement of the saturation broadening of the absorption profile as obtained by spectrally scanning the laser beam through the atom profile in the flame while monitoring the wavelength integrated fluorescence signal, i.e. by obtaining a *fluorescence excitation profile* [22]. If we assume that the laser is strictly monochromatic and spatially uniform and the atomic profile is characterized by purely homogeneous (Lorentzian) broadening, then it can be shown that

$$\delta\nu_{exc} = \delta\nu_L\left(1 + \frac{E}{E^{s-2L}}\right)^{1/2}. \tag{12}$$

Here, $\delta\nu_{exc}$ is the full width at half maximum of the experimentally measured fluorescence excitation profile, $\delta\nu_L$ is the full width at half maximum of the unperturbed Lorentzian function, E is the laser irradiance integrated over its linewidth and E^{s-2L} the saturation parameter. From Eqn (12), one can see that the plot of the experimentally observed $(\delta\nu_{exc})^2$ vs the laser integrated irradiance (or in this case vs the laser power, Φ, since a ratio of irradiances is concerned) should result in a straight line whose slope can provide the saturation parameter.

When the more realistic case of a gaussian laser profile and a gaussian atom profile is considered, the following relationship is obtained

$$\delta\nu_{exc} = \delta\nu'(\ln 2)^{-1/2}\left(\ln\frac{\Phi}{\Phi^{s-2L}}\right)^{1/2} \tag{13}$$

Here, $\delta\nu'$ represents the convolution of the laser and the atom bandwidths, and the other terms have been defined previously. From Eqn (13), one can see that the intercept of the line obtained by plotting $(\delta\nu_{exc})^2$ vs $\ln\Phi$ should give the saturation parameter. It is worth noting again that this last method is only valid if steady state conditions are warranted for the fluorescence signal. Experimentally, the influence of a third level can be manipulated to some extent in a vapour cell, where the pressure of the fill gas can be changed and the collisional population transfer between the levels changes as a result.

[20] H. P. HOOYMAYERS and C. TH. J. ALKEMADE, *J. Quant. Spectrosc. Radiat. Transfer* 6, 501 (1966).
[21] S. J. PEARCE, L. DE GALAN and J. D. WINEFORDNER, *Spectrochim. Acta* 23B, 793 (1968).
[22] N. OMENETTO, J. BOWER, J. BRADSHAW, C. A. VAN DIJK and J. D. WINEFORDNER, *J. Quant. Spectrosc. Radiat. Transfer* 24, 147 (1980).

Transient behavior of the fluorescence signal and the significance of the saturation parameter

As repeatedly pointed out in the preceding discussion, the fluorescence radiance was assumed to have reached steady state conditions during the measurement time. If the laser is pulsed and the duration of the pulse does not exceed a few nanoseconds, it can be questioned whether or not steady state conditions are warranted. The following considerations are intended to clarify and summarize some of the terminology used in the literature [1, 23–25] to define terms such as laser pumping time, system's response time and so on, as well as their mutual correlation. If a two level system (such as that of Fig. 2a) is subjected to a step-like excitation function, the solution of the differential equation set forth by simple balancing considerations for $n_3(t)$ gives

$$n_3(t) = n_3''(1 - e^{-t/t_r}). \tag{14}$$

Here, n_3'' is the steady state population of the excited level and t_r is the *response time* of the atomic system. This quantity is given in terms of source and atomic parameters by the following expression

$$t_r = \frac{1}{(1 + [g_1/g_3])c^{-1}E_{\nu_{13}}B_{13} + A_{31} + k_{31}}, \tag{15}$$

while the steady state population is given by

$$n_3'' = n_T E_{\nu_{13}} c^{-1} B_{13} t_r. \tag{16}$$

In both equations, all terms have been previously defined except for n_T which represents the total atomic population of the two levels ($n_1 + n_3$). The *pumping time* is defined as

$$t_p = \frac{c}{(1 + [g_1/g_3])B_{13}E_{\nu_{13}}}. \tag{17}$$

If one recalls the definition of the effective lifetime of the excited level, τ_{eff} (see Eqn (2), it is easy to see from Eqn (15) that the response time of the atomic system will be governed by the effective lifetime, τ_{eff}, or by the pumping time, t_p, depending upon the laser irradiance. If the population of the excited level is plotted vs time for increasing values of the laser irradiance, the characteristic curves shown in Fig. 3 result. These curves show that the response time of the system decreases when the laser irradiance increases. It is also clear that if we select from our detection system an infinitesimal gate width for the measurement of the fluorescence signal at the times t_1, t_2, t_3 and t_4, as indicated in Fig. 3, steady state will be obtained at *all* values of the laser irradiance *only at time* t_4. When the time at which the measurement is performed is set earlier in the response curve, then only at very high laser irradiances, i.e. when saturation is approached, steady state conditions are shown to exist. Although these considerations can be found in several literature references [1, 4, 5, 18], the implications concerning the evaluation of the saturation parameter have not been properly stressed, until recently [15]. In fact, it is now evident that only the fluorescence saturation curve obtained at time t_4 will give the correct estimate of the saturation spectral irradiance. If the measurement time is set at, for example, t_2, the *saturated* fluorescence values will be correct, but those obtained with the insertion of neutral density filters to decrease the laser irradiance will deviate more and more from the correct steady state values. Similar considerations hold for the measurements taken at times t_1 and t_3. As a

[23] A. P. Baronowski and J. R. McDonald, *Appl. Optics* **16**, 1897 (1977).
[24] R. P. Lucht and M. M. Laurendeau, *Appl. Optics* **18**, 856 (1979).
[25] D. Stepowski and M. J. Cottereau, *Appl. Optics* **18**, 354 (1979).

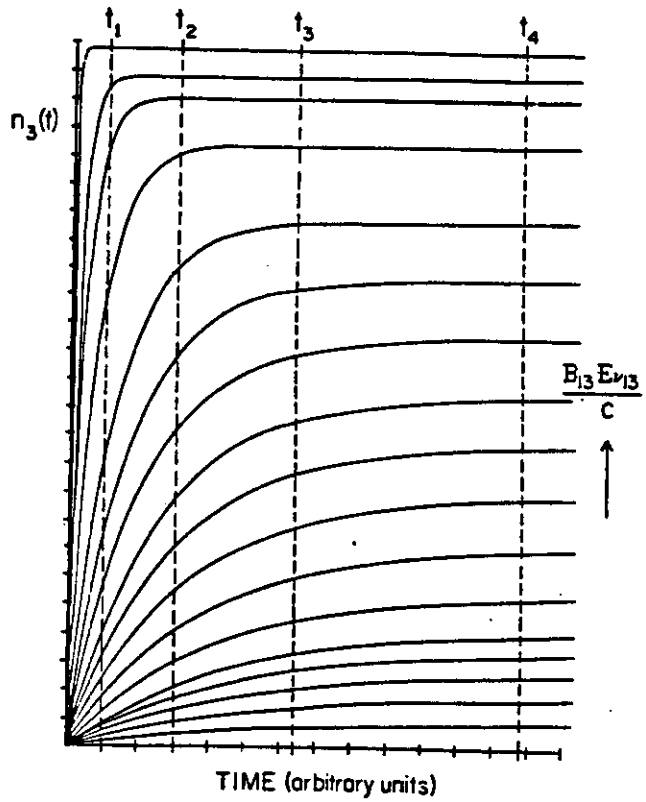

Fig. 3. Temporal behavior of the excited state population for a two level system under a steplike excitation pulse. Different curves correspond to different values of radiative pumping rates. Hypothetical measuring gates of infinitesimal width are indicated at t_1, t_2, t_3 and t_4.

result, as shown in Fig. 4, a *family* of fluorescence saturation curves will be obtained, all approaching the same saturation asymptote like the true curve, as it should be. However, the saturation parameter derived from these curves will be affected by a significant error. Figure 4 shows also that one cannot trust the procedure of deriving the saturation parameter (if the *full* saturation curve has not been drawn), from the

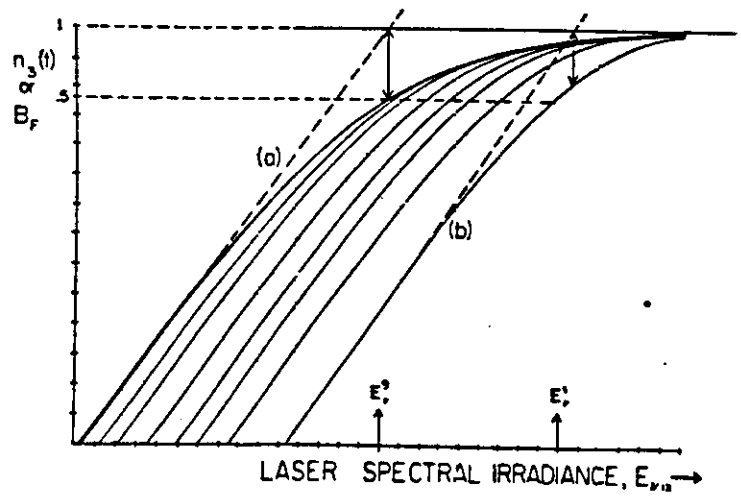

Fig. 4. Non steady state fluorescence saturation curves. Curves shown are obtained from Fig. 3, plotting the excited state population at the different times t_1, t_2, ... Curve (a), obtained at t_4, is the true steady state saturation curve. Curve (b) gives the worst value of the saturation parameters. As shown here, only for curve (a) the linear asymptote and the saturation asymptote intercept each other correctly. (Note that ordinate and abscissa are both logarithmic)

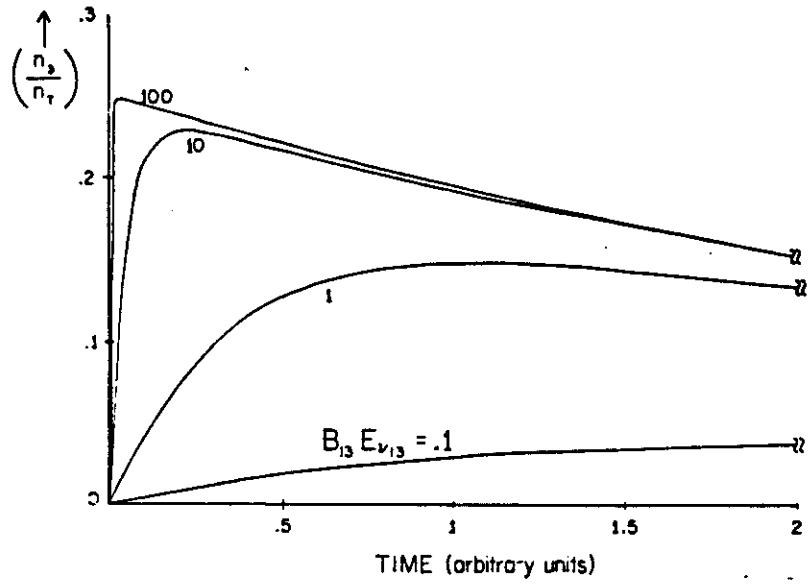

Fig. 5. Temporal behavior of the excited state population (fluorescence) for a three level system (thallium-type) where level 2 is considered as a sink ($k_{21} \ll k_{32} + A_{32}$). The different curves shown refer to different radiative pumping rates.

value obtained at the point where the linear asymptote reads twice the value of the saturation curve. On the other hand, this procedure proves to be a very reliable tool to check the validity of the saturation curve and of the measuring system.

Figure 4 has its experimental counterpart in practice if the laser pulse is considered to be approximated by rectangles whose leading edges are located at t_1, t_2, t_3 and t_4, respectively. Similar considerations hold for a three level system, when the differential equation for the temporal dependence of the population, solved for $n_3(t)$, gives

$$n_3(t) = n_3^{II}(C_1 e^{-t/\tau_3} + C_2 e^{-t/t_p} + 1) \tag{18}$$

where C_1 and C_2 are integration constants and τ_3 and t_p are the effective lifetimes of level 3 and the pumping time, respectively [1, 18, 26]. Figure 5 shows the temporal behavior of $n_3(t)$ at the very beginning of the excitation, for various laser pumping rates. It is clear that any measurement taken here aimed at evaluating the saturation parameter would be meaningless. Measurements must be taken at much later times (not shown in the figure) where the system has completely relaxed to steady state conditions and therefore true fluorescence saturation curves will be obtained.

Conclusions

The saturation spectral irradiance is a very useful quantity for the description of the saturation behavior of both atoms and molecules irradiated by an intense laser beam. Such parameters can be experimentally obtained in several ways, but most directly from the plot of the fluorescence signal vs the laser power. However, even for a two energy level systems, the saturation parameter can only be correctly defined and measured if steady state conditions are warranted. When the laser is pulsed, and the pulse duration is very short, it can be concluded that, although steady state is operative at saturation, the curve deviates from the true behavior as soon as the laser irradiance is decreased. As a consequence, serious experimental errors will occur.

Acknowledgements—Research supported by AFORS F49620-80C The computational skill of A. Colombo in plotting some of the figures is gratefully acknowledged.

[26] G. Zizak, J. D. Bradshaw and J. D. Winefordner, *Appl. Optics* **19**, 3631 (1980).

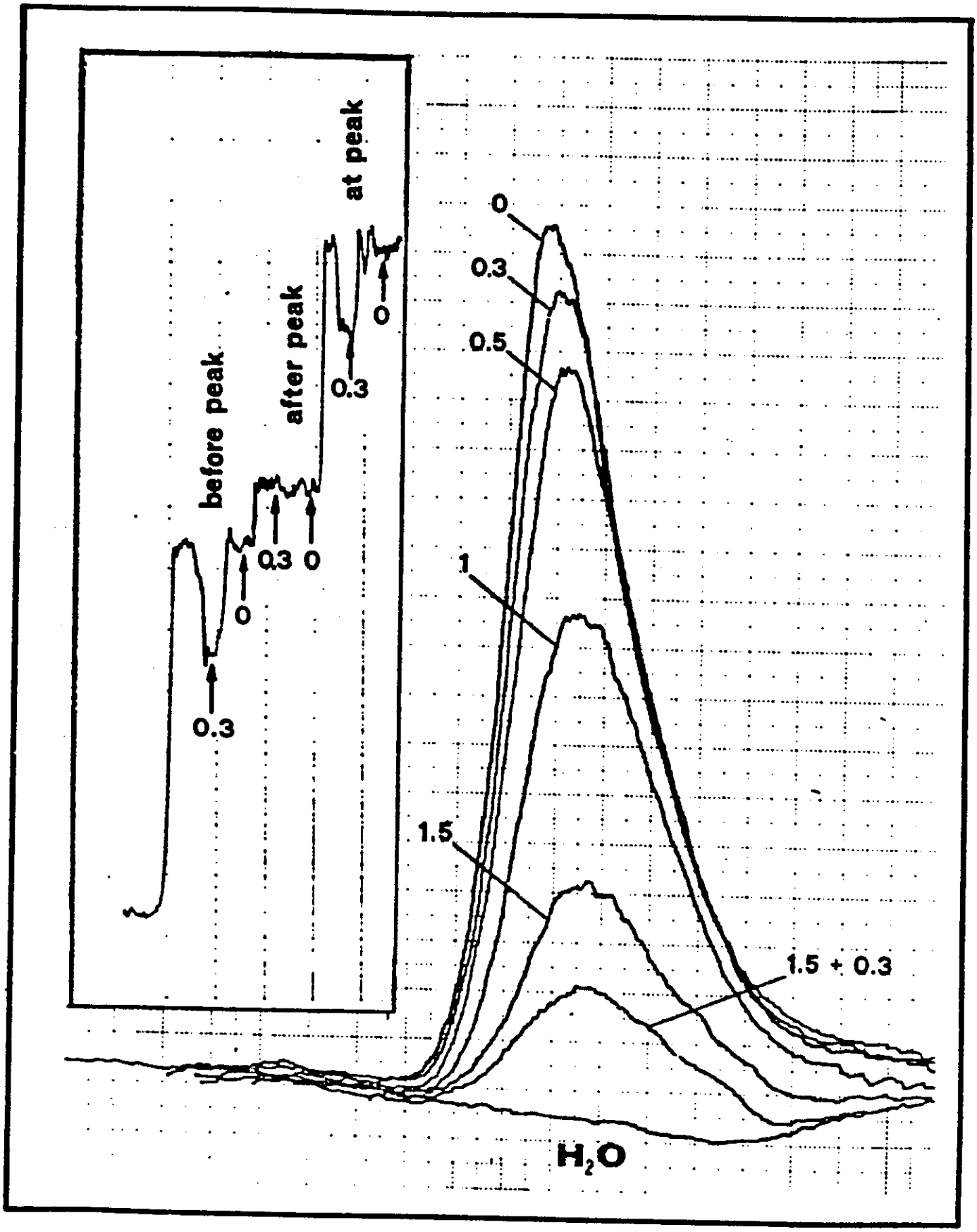
before peak
after peak
at peak
0.3
0
0.3
0
0.3
0
0
0.3
0.5
1
1.5
1.5 + 0.3
H2O

J. Quant. Spectrosc. Radiat. Transfer Vol. 24, pp. 147–158
Pergamon Press Ltd., 1980. Printed in Great Britain

A THEORETICAL AND EXPERIMENTAL APPROACH TO LASER SATURATION BROADENING IN FLAMES†

N. OMENETTO,‡ J. BOWER, J. BRADSHAW, C. A. VAN DIJK,§
and J. D. WINEFORDNER¶
Department of Chemistry, University of Florida, Gainesville, FL 32611, U.S.A.

(*Received* 26 *October* 1979)

Abstract—The broadening of the absorption profile in hydrogen-based flames diluted with argon and nitrogen is discussed theoretically and demonstrated experimentally with a pulsed tunable dye laser. This broadening is evaluated from the half-width of the profile obtained by scanning the laser beam through the atoms in the flame while monitoring the resulting fluorescence with a high luminosity monochromator, i.e. by observing a fluorescence excitation profile. Results are given for the elements Ca, Sr, Na, and In. It is shown that the halfwidth of the atomic profile depends approximately upon the square root of the log of the laser irradiance. This dependence stems from a theoretical treatment based upon the interaction of a gaussian laser profile and a gaussian atomic profile. It is also shown that if the laser spectral bandwidth exceeds by ≈5–10 times the absorption halfwidth, the fluorescence excitation profile provides a simple means for a reliable evaluation of the laser bandwidth.

INTRODUCTION

The high irradiance provided by the pulsed tunable dye laser is capable of saturating both single-photon and 2-photon transitions of atoms in flames at atmospheric pressure.[1–7] Among other effects, such as the attainment of the maximum fluorescence signal and its relative independence upon the quantum efficiency of the transition, the strong irradiation field is known to be responsible for a broadening of the absorption line profile. This broadening is called *saturation broadening*. Hosch and Piepmeier,[8] Van Dijk,[4] as well as others[9] reported an experimental verification of saturation broadening by performing both absorption and fluorescence measurements.

The aim of this work is to present a theoretical treatment of the saturation broadening based upon the rate equations approach and for the two cases of a very narrow excitation line laser coupled with a Lorentzian absorption profile and a Gaussian laser profile coupled with a Gaussian atom profile. The theoretical predictions will be compared with the experimental data obtained by scanning the laser beam throughout the atom profile in different flames while monitoring the fluorescence emitted at right angles, i.e. by obtaining a *fluorescence excitation profile*.[10,11]

We realize that our experimental conditions are not applicable to the first case (line source and Lorentzian atom profile). Furthermore, the second case (gaussian laser profile and gaussian atom profile) is certainly an approximation to the real interaction process. Nevertheless, we felt that it was useful to present our experimental data since the saturation broadening was clearly observed in all the cases investigated.

THEORY

The treatment given here follows the basic discussion on saturation which can be found in several books, chapters and articles.[1–7] Generally, atoms are considered to be dispersed as trace constituents in a gas at atmospheric pressure and characterized by a 2-level system. Coherence effects (cooperative phenomena) are neglected because dephasing, coherence-interrupting collisions are considered to be fast in our atmospheric pressure flames.[12,13]

†Work supported by AF-AFOSRF44620-78-C-0005 and by a Wright Patterson Air Force Base Contract AF-33615-78C-2036.

‡On leave from the Institute of Inorganic and General Chemistry, University of Pavia, Pavia, Italy.
§Post Doctoral Associate, Michigan State University, East Lansing, Michigan.
¶To whom all correspondence should be addressed.

Case A. Line source and Lorentzian atom profile

In this case, the laser is assumed to be a very narrow, monochromatic line source and the atomic absorption profile is considered to be homogeneously broadened. The first assumption can be met by tunable dye lasers.[14,15] Also, the laser beam is assumed to be spatially uniform. The case in which a Gaussian spatial profile is assumed for the radial dependence of the laser intensity[16,17] is discussed in the Appendix.

The atom profile can be considered homogeneous if the following conditions hold: (i) Doppler broadening is negligible compared to collisional broadening; (ii) in the case of combined Doppler and collisional broadening, velocity changing collisions are so fast that atoms cannot be considered to belong to any particular Doppler interval during the time of interaction with the laser beam.

Let the atoms be characterized by levels 1 and 2, with energy difference $h\nu_0$(J), statistical weights (dimensionless) g_1 and g_2 and number densities (m^{-3}) n^1 and n_2. The total atomic population in this case is $n_T = n_1 + n_2$. In the steady-state limit, we can obtain from a simple rate equations approach,[7] the following relationship:

$$\frac{n_2}{n_T} = \frac{B_{12}\{\rho(\lambda_l)/\delta\lambda_{eff}\}g^a(\lambda_l - \lambda_0)}{\left(1+\frac{g_1}{g_2}\right)(B_{12})\left(\frac{\rho(\lambda_l)}{\delta\lambda_{eff}}\right)g^a(\lambda_l - \lambda_0) + A_{21} + k_{21}}, \tag{1}$$

where B_{12} = Einstein coefficient of induced absorption, $J^{-1}\ m^3\ s^{-1}\ m$; A_{21} = Einstein coefficient of spontaneous emission, s^{-1}; k_{21} = collisional (quenching) rate constant, s^{-1}; $\rho(\lambda_l) \equiv \int_{\delta\lambda_l} \rho_\lambda(\lambda)\,d\lambda \equiv \rho_\lambda\,d\lambda_l$, integral energy density of the laser, integrated over the effective width of the laser line, $\delta\lambda_l$, in Jm^{-3}; $g_\lambda^a(\lambda_l - \lambda_0)$ = absorption shape function, given by the Lorentzian dispersion formula

$$g_\lambda^a(\lambda_l - \lambda_0) = \frac{1}{\pi}\left[\frac{\frac{\delta\lambda_L}{2}}{\left(\frac{\delta\lambda_L}{2}\right)^2 + (\lambda_l - \lambda_0)^2}\right], \quad m^{-1};$$

$\delta\lambda_L$ = full width at half maximum of the shape function, m; $1/\delta\lambda_{eff} \equiv g_\lambda^a(\lambda = \lambda_0) = 2/\pi\delta\lambda_L$, peak value of the shape function, m^{-1}; $\delta\lambda_{eff}$ = effective width of the absorption profile, m;

$$g^a(\lambda_l - \lambda_0) = \frac{g_\lambda^a(\lambda_l - \lambda_0)}{g_\lambda^a(\lambda = \lambda_0)} = g_\lambda^a(\lambda_l - \lambda_0)\left(\frac{\pi\delta\lambda_L}{2}\right), \text{ dimensionless.}$$

Equation (1) can be rewritten in terms of the effective lifetime, $\tau\ (\equiv A_{21} + k_{21})^{-1}$, of the excited level as

$$\frac{n_2}{n_T} = \frac{B_{12}\{\rho(\lambda_l)/\delta\lambda_{eff}\}g^a(\lambda_l - \lambda_0)\tau}{\left(1+\frac{g_1}{g_2}\right)B_{12}\{\rho(\lambda_l)/\delta\lambda_{eff}\}g^a(\lambda_l - \lambda_0)\tau + 1}. \tag{1a}$$

If the atomic density is low, then n_2 can be expressed in terms of the fluorescence radiance, B_F ($J\ s^{-1}\ m^{-2}\ sr^{-1}$), as

$$B_F = n_2\left(\frac{l}{4\pi}\right)A_{21}h\nu_0, \tag{2}$$

where l (m) is the homogeneous depth of the fluorescence volume in the direction of observation.

We now define the saturation energy density[1-7] as

$$\frac{\rho^s(\lambda_l)}{\delta\lambda_{eff}} \equiv \frac{A_{21} + k_{21}}{\left(1+\frac{g_1}{g_2}\right)B_{12}} \equiv \frac{1}{\left(1+\frac{g_1}{g_2}\right)B_{12}\tau} \equiv \frac{A_{21}}{\left(1+\frac{g_1}{g_2}\right)B_{12}Y_{21}}, \tag{3}$$

where $Y_{21} = \{A_{21}/(A_{21} + k_{21})\}$ is the quantum efficiency of the transition. By rearranging Eq. (1) and making use of Eqs. (2) and (3), we obtain for the atomic fluorescence radiance the following expression:

$$B_F = Cn_T \frac{\rho(\lambda_l)}{\rho^s(\lambda_l)} \left(\frac{g_2}{g_1 + g_2}\right) \frac{g^a(\lambda_l - \lambda_0)}{1 + \left(\frac{\rho(\lambda_l)}{\rho^s(\lambda_l)}\right) g^a(\lambda_l - \lambda_0)}, \tag{4}$$

where $C \equiv h\nu_0(l/4\pi)A_{21}$.

This equation shows the theoretical dependence of the wavelength integrated fluorescence radiance upon the laser energy density and the *detuning* between the peak of the laser profile, acting here as a delta function, and the peak of the Lorentzian atom absorption profile. It can be easily shown that this equation, in the low intensity limit, reduces to the well known linear dependence of the fluorescence radiance upon $\rho(\lambda_l)$ and Y_{21} while, in the high-intensity limit, n_2 becomes half of the total atomic population if the statistical weights are the same. This particular outcome holds, of course, irrespective of the line shape.

The ratio between braces in Eq. (4) is a modified Lorentzian function, which takes into account the effect of the laser field upon the spectral profile. The low intensity Lorentzian function can be written as

$$g^a(\lambda_l - \lambda_0) = \left(\frac{\pi\delta\lambda_L}{2}\right)\left[\frac{1}{\pi}\frac{\frac{\delta\lambda_L}{2}}{\left(\frac{\delta\lambda_L}{2}\right)^2 + (\lambda - \lambda_0)^2}\right], \tag{5}$$

while the modified Lorentzian function in Eq. (4) can be written as a function of the laser density ρ and the detuning $\delta \equiv (\lambda_l - \lambda_0)$ as follows:

$$g^a(\delta, \rho) = \left(\frac{\pi\delta\lambda_L}{2}\right)\left[\frac{1}{\pi}\frac{\frac{\delta\lambda_L}{2}}{\left(\frac{\delta\lambda_L}{2}\right)^2\left(1 + \frac{\rho(\lambda_l)}{\rho^s(\lambda_l)}\right) + \delta^2}\right]. \tag{6}$$

In both equations, $\delta\lambda_L$ is the full width at half maximum (FWHM) of the unperturbed Lorentzian function. Inspection of Eqs. (5) and (6) shows that the FWHM of the modified function, here called $\delta\lambda_{\text{excitation}}$, is given by

$$(\delta\lambda_{\text{exc}})^2 = (\delta\lambda_L)^2 + (\delta\lambda_L)^2\left(\frac{\rho(\lambda_l)}{\rho^s(\lambda_l)}\right) \tag{7a}$$

or

$$\delta\lambda_{\text{exc}} = \delta\lambda_L\sqrt{\left(1 + \frac{\rho(\lambda_l)}{\rho^s(\lambda_l)}\right)}. \tag{7b}$$

This equation shows that *the width of the absorption profile increases with the square root of the laser density.*

Several conclusions can be derived from Eq. (7).

(i) Since $\rho^s(\lambda_l)$ depends upon the quantum efficiency of the transition, the broadening effect at a fixed laser density will be *greater* in high quantum efficiency flames as compared to that observed in low quantum efficiency flames.

(ii) As indicated by Eq. (7a), a plot of the experimentally observed $(\delta\lambda_{\text{exc}})^2$ vs the laser density measured at the flame should result in a straight line. From the slope of this line, one can calculate the saturation density for that particular transition while from the intercept one can calculate the low intensity Lorentzian linewidth.

(iii) At the limit of $\rho(\lambda_l) = 0$, $\delta\lambda_{\text{exc}} = \delta\lambda_L$, as it should be.

(vi) Since the second term in the square root involves a ratio between the densities, one needs only to measure the laser power Φ, at the flame. Equation (7) can also be derived from

Eqs. (4) and (6) in the following manner. When the detuning in zero, the fluorescence signal is peaked at a value given by the following expression:

$$B_F(\delta = 0) = Cn_T\left(\frac{\rho(\lambda_l)}{\rho'(\lambda_l)}\right)\left(\frac{g_2}{g_1+g_2}\right)\frac{1}{1+\dfrac{\rho(\lambda_l)}{\rho'(\lambda_l)}}\ ; \tag{8}$$

when the detuning is very large, the fluorescence signal approaches zero. Therefore, we can find the detuning, $\delta^{\pm}_{1/2}$, at which the peak value of the function is halved, for both positive and negative detunings. We then have

$$\frac{1}{2}\ Cn_T\left(\frac{\rho(\lambda_l)}{\rho'(\lambda_l)}\right)\left(\frac{g_2}{g_1+g_2}\right)\left(\frac{1}{1+\dfrac{\rho(\lambda_l)}{\rho'(\lambda_l)}}\right)$$

$$= Cn_T\left(\frac{\rho(\lambda_l)}{\rho'(\lambda_l)}\right)\left(\frac{g_2}{g_1+g_2}\right)\left\{\frac{\left(\dfrac{\delta\lambda_L}{2}\right)^2}{\left(\dfrac{\delta\lambda_L}{2}\right)^2+\left(\dfrac{\delta\lambda_L}{2}\right)^2\left(\dfrac{\rho(\lambda_l)}{\rho'(\lambda_l)}\right)+(\delta_{1/2})^2}\right\}, \tag{9}$$

which gives

$$\delta\lambda_{exc} = (\delta)^{+}_{1/2} - (\delta)^{-}_{1/2} = \delta\lambda_L\sqrt{\left(1+\frac{\rho(\lambda_l)}{\rho'(\lambda_l)}\right)} \tag{10}$$

and is seen to be identical with Eq. (7).

Case B. *Gaussian laser profile and Gaussian atom profile*

This case can be considered to be closer to our experimental set-up when the pulsed laser beam is not very narrow and the atom profile in the flame is described by a Voigt profile. Here, the laser is assumed to Gaussian so that its spectral energy density ($J\,m^{-3}\,m^{-1}$) is given by the following expression:

$$\rho_\lambda(\lambda) = \rho\frac{2\sqrt{(\ln 2)}}{\sqrt{(\pi)}\delta\lambda_l}\exp-\left\{\frac{2\sqrt{(\ln 2)}}{\delta\lambda_l}(\lambda-\lambda_l)\right\}^2, \tag{11}$$

where ρ is the integrated energy density ($J\,m^{-3}$) and $\delta\lambda_l$(m) is the FWHM of the laser spectral profile. Accordingly, the atom profile is given by the following dimensional (m^{-1}) shape function:

$$g_\lambda{}^a(\lambda-\lambda_0) = \frac{2\sqrt{(\ln 2)}}{\sqrt{(\pi)}\delta\lambda_a}\exp-\left\{\frac{2\sqrt{(\ln 2)}}{\delta\lambda_a}(\lambda-\lambda_0)\right\}^2, \tag{12}$$

where $\delta\lambda_a$ is now the FWHM of the atom spectral profile. As stated before, the atoms here are not considered to be grouped in Doppler intervals (which would cause hole burning for a spectrally narrow, saturating laser beam) because of the very effective cross-relaxation taking place in the flame. The interaction of the laser and the atoms in Eq. (4) is now given by the convolution integral of both profiles. Since the convolution of two Gaussian functions is still a Gaussian function, we obtain

$$\int \rho_\lambda(\lambda)g_\lambda{}^a(\lambda-\lambda_0)\,d\lambda = \rho\frac{2\sqrt{(\ln 2)}}{\sqrt{(\pi)}\delta\lambda'}\exp-\left\{\frac{2\sqrt{(\ln 2)}}{\delta\lambda'}(\lambda_l-\lambda_0)\right\}^2, \tag{13}$$

where $(\lambda_l-\lambda_0)$ is the detuning between the centers of both profiles and $\delta\lambda'$ represents the convolution of the laser and the atom halfwidths, i.e.

$$\delta\lambda' \equiv \sqrt{[(\delta\lambda_l)^2+(\delta\lambda_a)^2]}. \tag{14}$$

Proceeding as before and defining now the saturation spectral density as

$$\rho^s = \frac{\delta\lambda'\sqrt{\pi}}{\left(1+\frac{g_1}{g_2}\right)B_{12}\tau 2\sqrt{(\ln 2)}}, \tag{15}$$

we obtain for the halfwidth of the fluorescence excitation profile

$$\delta\lambda_{exc} = (\delta)^{+}_{1/2} - (\delta)^{-}_{1/2} = \frac{\delta\lambda'}{\sqrt{(\ln 2)}}\sqrt{\left(\ln\left(2+\frac{\rho}{\rho^s}\right)\right.}. \tag{16}$$

where all of the terms have been previously defined.

Several conclusions can be drawn from Eq. (15):

(i) High quantum efficiency flames will be more sensitive for the observation of the broadening effect, exactly as in the preceding case.

(ii) In this case, saturation broadening sets in at a *lower* rate as compared to the previous case (narrow line and Lorentzian atom profile).

(iii) At the limit, when $\rho \to 0$, $\delta\lambda_{exc} \to \delta\lambda'$, as it should be.

(iv) If the value of the laser density greatly exceeds the saturation energy density for that particular transition, the 2 can be neglected in the argument of the logarithm and Eq. (16) can be written as

$$\delta\lambda_{exc} = \frac{\delta\lambda'}{\sqrt{(\ln 2)}}\sqrt{\left(\ln\frac{\phi}{\phi^s}\right)} \tag{17}$$

or

$$(\delta\lambda_{exc})^2 = \frac{(\delta\lambda')^2}{\ln 2}\{\ln\phi - \ln\phi^s\}, \tag{18}$$

where ϕ and ϕ^s correspond to ρ and ρ^s but are fluxes, in J s^{-1} m^{-2}. From Eq. (18), one can see that, by plotting $(\delta\lambda_{exc})^2$ vs ln ϕ, a straight line is obtained. The slope of this line gives $\delta\lambda$, while the intercept gives ϕ^s.

EXPERIMENTAL

The experimental set-up used is described in detail elsewhere.[18] The tunable dye laser (DL-400, Molectron, Sunnyvale, CA) pumped by a nitrogen laser (UV-14, Molectron, Sunnyvale, CA) is directed into the flame by means of two plane mirrors after passing through two spatial filters consisting of shielded iris diaphragms (Edmund Scientific, Barrington, N.J.). These filters passed only the central portion of the beam so as to improve its uniformity. No lenses were placed between the iris and the flame. The flame used was an oxygen–hydrogen mixture diluted with argon or nitrogen, and supported by a capillary burner. For these measurements, the flame was surrounded by a gas sheath (Ar or N_2) but was not protected by a similar analyte-free flame burning at the same composition and temperature. All measurements were taken at approximately 1 cm above the primary reaction zone. The standard solutions for all elements (Ca, Sr, Na, and In) were made from reagent grade chemicals. The concentration was chosen to be very low to avoid any self-absorption, pre-filter or post-filter effects.

The fluorescence was collected at right angles by an optical system consisting of two spherical quartz lenses and a rectangular aperture. The flame was imaged at unit magnification onto this aperture and after that, with the same magnification, onto the entrance slit of a high luminosity monochromator (Jobin Yvon, model H-10, 10-cm focal length, f-3.6) whose slit width was set for all elements at 0.5 mm. The signal from a photomultiplier wired for fast pulse high current work and operated at −1000 V was processed by a dual channel boxcar integrator (model 162–164, PAR, Princeton, New Jersey). In order to sample only a small portion of the fluorescence waveform, which in our case is the result of the saturation process and the photomultiplier temporal characteristics,[18] we have used a 75-ps risetime sampling head (PAR

Model 163 sampled integrator). The monochromator was centered at the peak of the fluoresence line and the laser output was slowly scanned across the absorption profile. These measurements were then repeated by decreasing the laser irradiance with calibrated neutral density filters. Particular care was taken to minimize spurious reflections and scatter of the laser into the monochromator.

The peak power of the laser at the particular transition used was measured with a calibrated photodiode (Model F4000, ITT, Fort Wayne, Indiana) coupled directly to a scope (Type 454, Tektronix, Portland, Oregon).

The laser spectral bandwidth was measured directly with a good resolution grating monochromator (Jobin Yvon, MODEL HR-1000, 1-m focal length, f-5.4). The spectral slit function of such monochromator, evaluated by scanning a very low pressure mercury pen light in front of it, was found to be 0.12 Å.

RESULTS AND DISCUSSION

Figures 1–4 show clearly the broadening effect on the line profile as the laser irradiance on the atoms increases. The broadening in the halfwidth ranges from a factor of 1.3 for In to 5.4 for Sr. Obviously, as expected and stated before, this broadening cannot be accounted for by Eq. (7b) which was derived with the assumption of a monochromatic laser and a Lorentzian atom profile. Indeed, since in some cases (Sr and Ca), the laser power exceeded the saturation power by approximately a factor of 100, Eq. (7b) would have predicted a 10-fold broadening of the profile. Except for the case of indium (Fig. 1) for which a 15 ns boxcar gate width was used to average the signal, the profiles have been obtained with the 75 ps risetime sampling head. This explains the different noise levels shown in the figures.

Irrespective of the theoretical assumptions made, both Eq. (7) and (16) predict a larger broadening effect with high quantum efficiency flames as compared with that observed with low quantum efficiency flames. Despite the fact that our flames are not shielded (apart from an outer gas sheath), the replacement of argon as diluent by nitrogen should change considerably the quantum efficiency. Thus, different broadenings are expected for the same laser power but for the two flames. The experimental results, collected in Table 1, do indeed show the correct trend, with the exception of strontium. These values are therefore indicative of the different

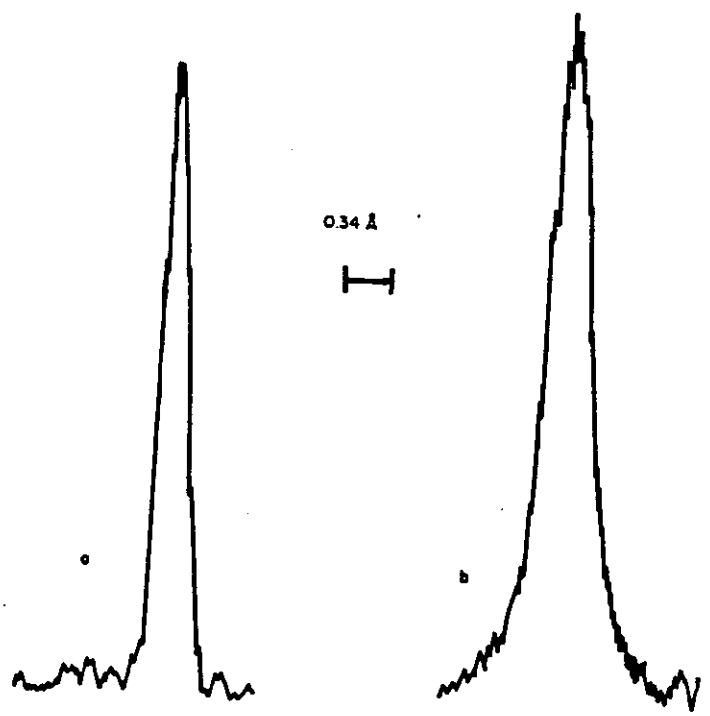

Fig. 1. Fluorescence excitation profiles for indium in the Ar–O_2–H_2 flame. Resonance fluorescence at 4101 Å; abscissa: Å; indium concentration, 100 μg/mL; (a) laser power: 0.37 kW; $\delta\lambda_{exc} = 0.19$ Å; (b) laser power: 3.7 kW; $\delta\lambda_{exc} = 0.37$ Å.

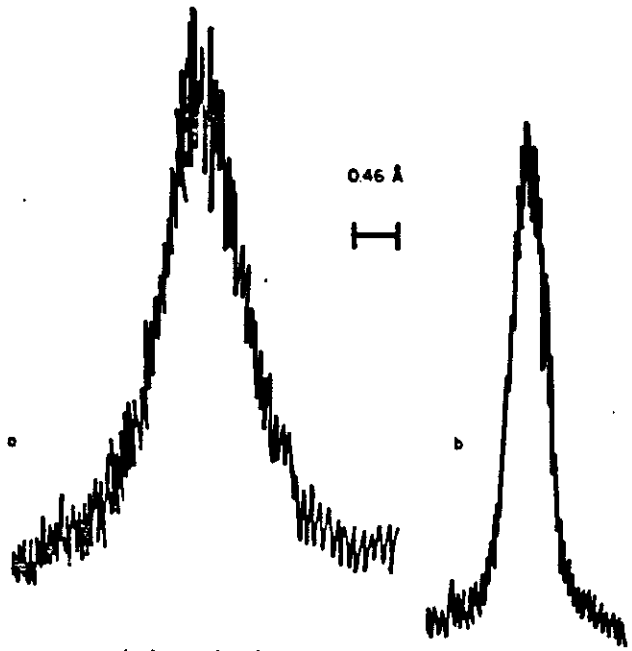

Fig. 2. Fluorescence excitation profiles for sodium in the $Ar–O_2–H_2$ flame; the resonance fluorescence is shown at 5890 Å; abscissa: Å; sodium concentration, 10 μg/mL; (a) laser power: 17 kW; $\delta\lambda_{exc} = 0.99$ Å; (b) laser power: 1.7 kW; $\delta\lambda_{exc} = 0.46$ Å.

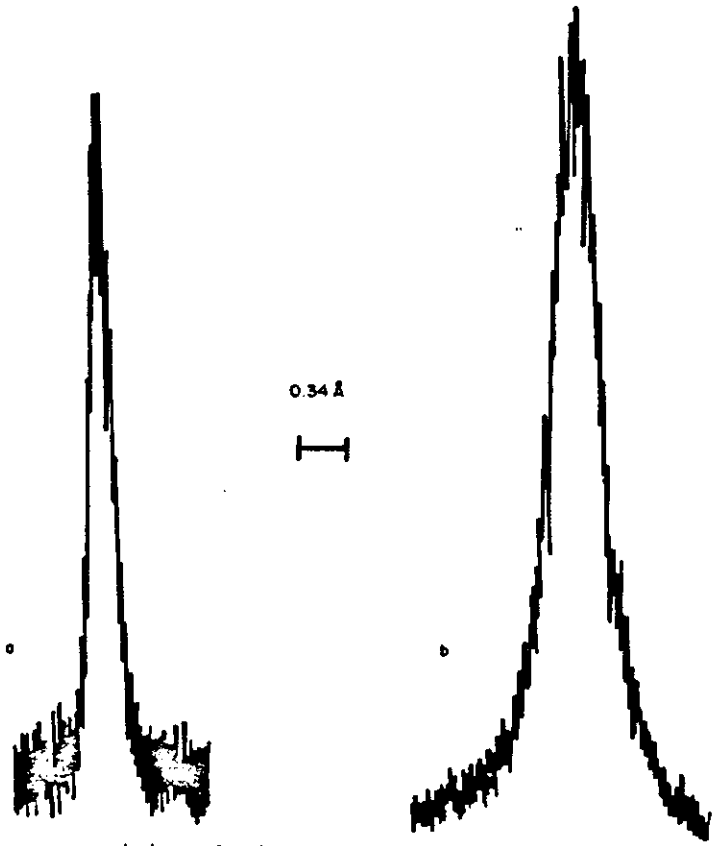

Fig. 3. Fluorescence excitation profiles for calcium in the $N_2–O_2–H_2$ flame; resonance fluorescence at 4227 Å, abscissa: Å calcium concentration, 10 μg/mL; (a) laser power: 50W; $\delta\lambda_{exc} = 0.20$ Å; (b) laser power: 5 kW; $\delta\lambda_{exc} = 0.44$ Å.

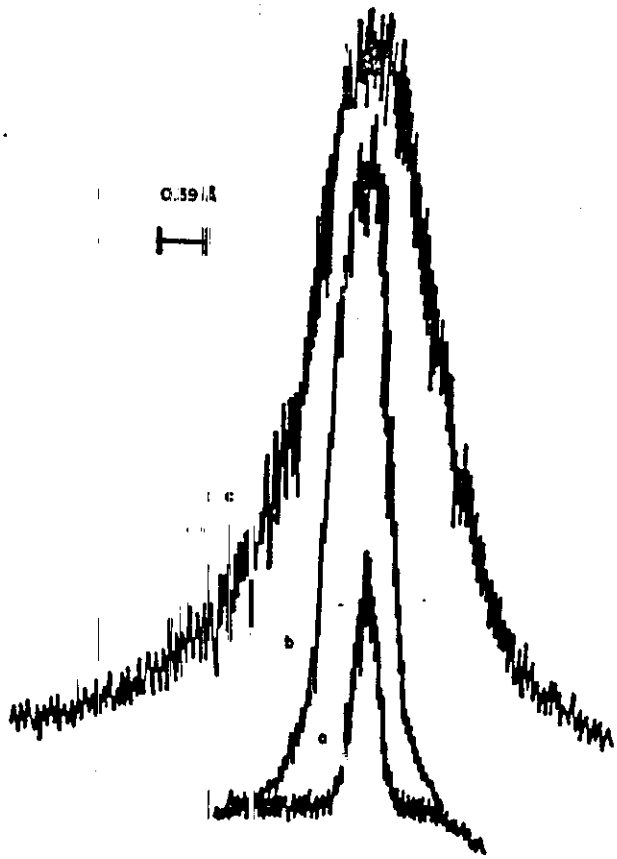

Fig. 4. Fluorescence excitation profiles for strontium in the N_2–O_2–H_2 flame; resonance fluorescence at 6407 Å; strontium concentration 1 μg/mL. (a) laser power: 14W; $\delta\lambda_{exc} = 0.23$ Å; (b) laser power 1.4 kW; $\delta\lambda_{exc} = 0.55$ Å; (c) 14 kW; $\delta\lambda_{exc} = 1.25$ Å.

quantum efficiency and, in turn, of the different saturation powers in the two flames. This matter is discussed in greater details in another paper.[19]

In an attempt to compare the experimental data with the theoretical predictions given by Eq. (16), we have calculated for both flames the ratio between the maximum value of $\delta\lambda_{exc}$ (corresponding to that obtained at full laser power) and the minimum value of $\delta\lambda_{exc}$ (corresponding to that obtained at $\rho \ll \rho^s$, i.e. when $\delta\lambda_{exp} \simeq \delta\lambda'$. The saturation power was evaluated for each element from the experimental saturation curve.[19] In Table 2, we compare this ratio with those obtained experimentally, where the values for $(\delta\lambda_{exc})_{min}$ are those obtained at very low laser powers (see also Table 3). Apart from some unexplained discrepancies outside the

Table 1. Experimental values of the saturation-broadened half-widths obtained for Ar–O_2–H_2 and the N_2–O_2–H_2 flames. *)

Element	δλ (Å)	
	$Ar/O_2/H_2$	$N_2/O_2/H_2$
Ca	0.51	0.44
Sr	1.24	1.25
Na	0.99	0.63
In	0.44	0.36

(*) All values are within ± 10%. Laser power: Ca, 5kW; Sr, 14kW; Na, 17kW; In, 7kW.

Table 2. Comparison between the theoretical and the experimental values of the fluorescence excitation profile half-widths for $Ar–O_2–H_2$ and $N_2–O_2–H_2$ flames. (a)

Element	$[(\delta\lambda_{exc})_{max}/(\delta\lambda_{exc})_{min}]$ (b)			
	Theoretical (c)		Experimental	
	$Ar/O_2/H_2$	$N_2/O_2/H_2$	$Ar/O_2/H_2$	$N_2/O_2/H_2$
Ca	2.5	2.4	3.0	2.2
Sr	2.8	2.8	2.9	5.4
Na	2.4	2.0	4.3	1.6
In	1.7	1.4	2.3	1.3

(a) values are considered to be within ± 10%.

(b) $(\delta\lambda)_{max}$ refers to the value obtained with the laser at full power while $(\delta\lambda)_{min}$ refers to that obtained when the laser is attenuated with neutral density filters until the fluorescence signal is linearly related to the laser irradiance (see values reported in Table 3).

(c) calculated according to Equation 16 in the text.

Table 3. Comparison between the values of the laser spectral bandwidth as obtained by different methods. (a)

Element	$\delta\lambda$ (Å)				
	Direct (b) Measurement	Fluorescence (c) Excitation Profile		Saturation (d) Broadening	
		$Ar/O_2/H_2$	$N_2/O_2/H_2$	$Ar/O_2/H_2$	$N_2/O_2/H_2$
Ca	0.23	0.20	0.20	0.26	0.21
Sr	0.23	0.42	0.23	0.46	0.51
Na	0.36	0.23	0.40	0.30	0.35
In	0.24	0.19	0.28	0.26	0.21

(a) values are within ± 10%.

(b) values obtained by scanning the laser beam thpough a 1-m grating monochromator ($\Delta\lambda$ resolution = 0.12 Å). Values are not corrected for the instrumental profile.

(c) values obtained by scanning the attenuated laser beam through the atomic vapor in the flame.

(d) values calculated from the slope of the plot obtained from Equation 16 in the text.

range of the experimental errors (such as the experimental value for strontium in the nitrogen-diluted flame), the agreement between the theory and the experiment can be considered fairly satisfactory, when all the assumptions made at the beginning are properly and critically considered.

In the flames used in this work, the halfwidth of the atom profile is expected to be of the order of 0.05 Å for all the elements considered. Therefore, the convolution obtained by scanning the laser through the absorption profile at low laser powers can be practically entirely attributed to the laser spectral halfwidth. For our theory to be consistent, the values so obtained (fluorescence excitation profile) should be the same as those given by the slope of the plot of Eq. (16), as explained before. Table 3 shows the different values obtained with these two methods. In addition, the values obtained by measuring directly the laser profile with a medium resolution monochromator are also shown. Again, apart from some differences, the average value for the two flames obtained with both techniques (fluorescence excitation profile and saturation broadening) closely agrees with that measured directly. We therefore feel that, whenever the laser bandwidth exceeds by approx. 5–10 times the atom profile, the halfwidth obtained from the low intensity fluoresence excitation profile provides a reliable estimate of the laser spectral bandwidth. Obviously, this method fails when the laser bandwidth is much narrower than the atom profile (since in this case the convolution will be essentially given by the atom profile) and loses its significance when the laser bandwidth is much larger (>20 times) than the atom profile. In this last case, it would be indeed much simpler to scan the laser directly through a small-medium resolution monochromator.

CONCLUSIONS

As stated at the beginning, it was not the purpose of this work to find a theoretical treatment of the saturation broadening that would perfectly fit our experimental conditions. In fact, in order to do this, the exact spectral shape of the laser pulse and the atom profile have to be known. Nevertheless, we feel that the results obtained are useful and can, at least qualitatively, be explained by our theoretical approach.

The main results of this work may be summarized as follows:

(i) As has been known theoretically and shown experimentally before,[1–9] the atomic profile broadens when the laser irradiance is such that saturation can be approached.

(ii) The broadening effect is larger for higher quantum efficiency flames.

(iii) For a pulsed, tunable dye laser (without spectral narrowing elements in the cavity), pumped by a nitrogen laser and a flame at atmospheric pressure, the broadening depends approximately upon the square root of the log of the laser irradiance.

(iv) The halfwidth of the fluorescence excitation profile obtained at low laser powers can indeed be taken as a measurement of the laser spectral bandwidth if this bandwidth is approx. 5–10 times larger than the atom profile.

REFERENCES

1. R. H. Pantell and H. E. Putoff, *Fundamentals of Quantum Electronics*. Wiley, New York (1969).
2. N. Omenetto [Ed.], *Analytical Laser Spectroscopy*. Wiley, New York (1979).
2a. C. Th. J. Alkemade, Plenary Lecture given at the *3rd Int. Conf. on Atomic Specroscopy*, Toronto (1973).
2b. C. Th. J. Alkemade, Plenary Lecture given at the *5th Int. Conf. on Atomic Spectroscopy*, Prague (1977).
3. E. H. Piepmeier, *Spectrochim. Acta* 27B, 431 (1972).
3a. E. H. Piepmeier, *Spectrochim. Acta* 27B, 445 (1972).
4. C. A. Van Dijk, Ph.D. Dissertation, Utrecht (1978).
5. N. Omenetto, P. Benetti, L. P. Hart, J. D. Winefordner, and C. Th. J. Alkemade, *Spectrochim. Acta* 28B, 289 (1973).
6. R. A. Van Calcar, M. J. M. Van de Ven, B. K. Van Uitert. K. J. Biewenga, Tj. Hollander, and C. Th. J. Alkemade, *JQSRT* 21, 11 (1979).
7. N. Omenetto and J. D. Winefordner, *Progress in Analytical Atomic Spectroscopy*, Vol. 2 (1, 2). Pergamon Press, Oxford (1979).
8. J. W. Hosch and E. H. Piepmeier, *Appl. Spectroscopy* 32, 444 (1978).
9. S. Ezekiel and F. Y. Wu, In *Multiphoton Processes* (Edited by J. H. Eberly and P. Lambropoulos). Wiley, New York (1978).
10. C. Th. J. Alkemade and T. Wijchers, *Anal. Chem.* 49, 2111 (1977).
11. R. A. Keller and J. C. Travis, *Analytical Laser Spectroscopy* (Edited by N. Omenetto), Chap. 8. Wiley, New York (1979).
12. H. P. Hooymayers and C. Th. J. Alkemade, *JQSRT* 6, 847 (.966).
13. J. W. Daily, *Appl. Opt.* 18, 360 (1979).
14. H. Walther, In *Multiphoton Processes* (Edited by J. H. Eber y and P. Lambropoulos), Wiley, New York (1978).

15. F. Y. Wu, R. E. Grove, and S. Ezekiel, *Phys. Rev. Lett.* **35**, 1426 (1975).
16. A. B. Rodrigo and R. M. Measures, *IEEE QE* **9**, 972 (1973).
17. J. W. Daily, *Appl. Opt.* **17**, 225 (1978).
18. J. D. Bradshaw, N. Omenetto, J. N. Bower, and J. D. Winefordner, *Spectrochim. Acta B*, submitted.
19. J. N. Bower, N. Omenetto, J. D. Bradshaw, and J. D. Winefordner, *Spectrochim. Acta B*, submitted.

Acknowledgements—N. Omenetto would like to thank the Committee for the International Exchange of Scholars for the grant of a Fulbright travel fellowship.

APPENDIX

Derivation of Eq. (16) *by taking into account some spatial inhomogeneity of the laser beam*

If the laser beam is not uniform, as assumed in our derivation, its spatial energy density profile can be represented again by a gaussian expression as

$$\rho = \rho_0 \exp - \left(\frac{2\sqrt{(\ln 2)}r}{\delta_r}\right)^2. \tag{A1}$$

where ρ_0 is now the integrated energy density at the peak of *both* the wavelength profile and the radial profile, $r(0 \le r \le \infty)$ is the radial coordinate and δ_r is the spatial full width at half maximum of the beam. In this case, the interaction of the laser and the atoms, as given by Eq. (13), has to be modified to include the spatial dependence of the laser density.[16,17] We therefore find for the ratio of the atom densities the following expression:

$$\frac{n_2}{n_T} = \frac{B_{12}\tau \dfrac{2\sqrt{(\ln 2)}}{\sqrt{(\pi)}\delta\lambda'} \exp - \left[\dfrac{2\sqrt{(\ln 2)}}{\delta\lambda'}(\lambda_l - \lambda_0)\right]^2 \rho_0 \exp - \left(\dfrac{2\sqrt{(\ln 2)}}{\delta_r} r\right)^2}{\left(1 + \dfrac{g_1}{g_2}\right) B_{12}\tau \dfrac{2\sqrt{(\ln 2)}}{\sqrt{(\pi)}\delta\lambda'} \exp - \left[\dfrac{2\sqrt{(\ln 2)}}{\delta\lambda'}(\lambda_l - \lambda_0)\right]^2 \rho_0 \exp - \left(\dfrac{2\sqrt{(\ln 2)}}{\delta_r}\right)^2 + 1} \tag{A2}$$

which can be written in a simplified form as

$$\frac{n_2}{n_T} = \frac{B_{12}\tau g(\delta\lambda)\rho_0 \exp - (cr)^2}{\left(1 + \dfrac{g_1}{g_2}\right) B_{12}\tau g(\delta\lambda)\rho_0 \exp - (cr)^2 + 1}, \tag{A3}$$

where

$$g(\delta\lambda) = \frac{2\sqrt{(\ln 2)}}{\sqrt{(\pi)}a\lambda'} \exp - \left[\frac{2\sqrt{(\ln 2)}}{\delta\lambda'}(\lambda_l - \lambda_0)\right]^2, \quad c = \frac{2\sqrt{(\ln 2)}}{\delta_r}.$$

If we now proceed as in the text, introducing the saturation spectral energy density given by Eq. (15), we obtain

$$\frac{n_2}{n_T} = \left(\frac{g_2}{g_1 + g_2}\right)\left(\frac{\exp - (cr)^2}{\exp - (cr)^2 + R(\delta\lambda)}\right). \tag{A4}$$

where $R(\delta\lambda) = \rho'/\rho_0$.

Assuming the usual vertical monochromator slit arrangement (cylindrical volume) and a proportional variation of n_2 vs r according to the laser variation, the ratio in Eq. (A4) can be integrated over r as follows:[17]

$$\frac{n_2}{n_T} = \int_0^\infty \frac{\exp - (cr)^2}{\exp - (cr)^2 + R(\delta\lambda)} 2\pi r \, dr. \tag{A5}$$

where the integration limit is extended to infinity since the slit height is much larger than the beam diameter. By solving the integral, we obtain

$$\frac{n_2}{n_T} = \frac{\pi}{c^2} \ln\left[1 + \frac{1}{R(\delta\lambda)}\right]. \tag{A6}$$

Evaluating $\delta\lambda_{exc}$ according to the procedure adopted in the main text, we obtain

$\delta\lambda_{exc}$ according to the procedure adopted in the main text, we obtain

$$\delta\lambda_{exc} = (\delta)^+_{1/2} - (\delta)^-_{1/2} = \frac{\delta\lambda'}{\sqrt{(\ln 2)}} \sqrt{\left(\ln\left[\frac{\rho_0}{\rho'(\sqrt{[1 + (\rho_0/\rho')]} - 1)}\right]\right)}. \tag{A7}$$

which can be written as

$$\delta\lambda_{exc} = \frac{\delta\lambda'}{\sqrt{(\ln 2)}} \sqrt{\left(\ln \frac{\chi}{\sqrt{(1+\chi)} - 1}\right)}. \tag{A8}$$

where $\chi = (\rho_0/\rho')$.

In conclusion, if we compare Eq. (A8) with Eq. (16), we can see that the spatial averaging effects, if present, tend to *lessen the dependence of the broadening of the spectral atom profile upon the laser power.* The effect will of course be more pronounced if the laser beam is focused in the flame so as to reach high irradiances. However, even in the presence such effect, the value of $\delta\lambda'$, as obtained from Eq. (A8), is the same as that given by Eq. (16).